Science Bulletin 70 (2025) 3614–3624

Contents lists available at ScienceDirect

Science Bulletin

journal homepage: www.elsevier.com/locate/scib

Article

The lifespan trajectories of brain activities related to conflict-driven cognitive control

Zhenghan Li [a,b,c], Isaac T. Petersen [d], Lingxiao Wang [e,f,g], Joaquim Radua [h,i,j], Guochun Yang [k,l,m,*], Xun Liu [m,n]

[a] Zhejiang Philosophy and Social Science Laboratory for Research in Early Development and Childcare, Hangzhou Normal University, Hangzhou 311121, China
[b] Institute of Brain Science and Department of Physiology, School of Basic Medical Sciences, Hangzhou Normal University, Hangzhou 311121, China
[c] Department of Psychology, Jing Hengyi School of Education, Hangzhou Normal University, Hangzhou 311121, China
[d] Department of Psychological and Brain Sciences, University of Iowa, Iowa City, IA 52242, USA
[e] Centre for Cognition and Brain Disorders/Department of Neurology, The Affiliated Hospital of Hangzhou Normal University, Hangzhou 311121, China
[f] Institute of Psychological Science, Hangzhou Normal University, Hangzhou 311121, China
[g] Zhejiang Key Laboratory for Research in Assessment of Cognitive Impairments, Hangzhou 311121, China
[h] Institut d'Investigacions Biomèdiques August Pi i Sunyer (IDIBAPS), CIBERSAM, University of Barcelona, Barcelona 08036, Spain
[i] Institute of Psychiatry, Psychology and Neuroscience, King's College London, London WC2R 2LS, UK
[j] Department of Clinical Neuroscience, Karolinska Institute, Stockholm 17177, Sweden
[k] Guangdong Institute of Intelligence Science and Technology, Zhuhai 519031, China
[l] Cognitive Control Collaborative, University of Iowa, Iowa City, IA 52242, USA
[m] Institute of Psychology, Chinese Academy of Sciences, Beijing 100101, China
[n] Department of Psychology, University of Chinese Academy of Sciences, Beijing 101408, China

ARTICLE INFO

Article history:
Received 17 March 2025
Received in revised form 12 June 2025
Accepted 18 August 2025
Available online 23 August 2025

Keywords:
Cognitive control
Lifespan trajectories
Brain activities
Neuroimaging meta-analysis
Inverted U-shape

ABSTRACT

Cognitive control is fundamental to human goal-directed behavior. Understanding its trajectory across the lifespan is crucial for optimizing cognitive function throughout life, particularly during periods of rapid development and decline. While existing studies have revealed an inverted U-shaped trajectory of cognitive control in both behavioral and anatomical domains, the age-related changes in functional brain activities remain poorly understood. To bridge this gap, we conducted a comprehensive meta-analysis of 139 neuroimaging studies using conflict tasks, encompassing 3765 participants aged 5 to 85 years. We adopted the seed-based d mapping (SDM), generalized additive model (GAM), and model comparison approaches to investigate age-related changes in brain activities to characterize the lifespan trajectories of cognitive control. Our analyses revealed two key findings: (1) The predominant lifespan trajectory is inverted U-shaped, rising from childhood to peak in young adulthood (between 27 and 36 years) before declining in later adulthood; (2) Both the youth and the elderly show weaker brain activities and greater left laterality than young adults. These results collectively reveal the lifespan trajectories of cognitive control, highlighting systematic fluctuations in brain activities with age.

1. Introduction

Many cognitive abilities of human beings dynamically change throughout the entire lifespan, experiencing rapid development in the early stages, and gradual decline in the later period of life. As one of the most fundamental cognitive functions, cognitive control is deeply engaged in various domains of high-level capabilities that humans greatly outperform other species, such as decision making, planning, and problem-solving [1]. Cognitive control refers to the cognitive processes that enable individuals to manage and regulate their attention, thoughts, and actions, which play a vital role in goal-directed behavior, allowing us to focus on the target and ignore distractors [2]. For instance, cognitive control enables us to concentrate on reading in a library despite the presence of people chatting nearby.

Cognitive control provides fundamental support for normal human behaviors. Young adults typically maintain an optimal mature level of cognitive control [3]. However, the youth (including children and adolescents, less than 18 years) and elderly (60 years and older) individuals may struggle with behavioral problems because of their suboptimal cognitive control system [4,5]. While the state-of-art progress of cognitive/behavioral changes has been well-documented and shaped the diagnosis criteria for developmental/aging-related disorders [6], the change of related neural systems has been under-investigated. Understand-

* Corresponding author.
E-mail address: yangguochun@gdiist.cn (G. Yang).

https://doi.org/10.1016/j.scib.2025.08.038
2095-9273/

ing how the neural underpinning of cognitive control changes over the lifespan can yield valuable insights into the developmental and ageing mechanisms of the human brain. This knowledge may assist in customizing cognitive training strategies based on related brain regions and their activities [7].

Researchers generally believe that cognitive control ability follows an inverted U-shaped trajectory across the lifespan [4,8]. This inverted U-shaped trajectory has been generally supported by behavioral and anatomical evidence. The Eriksen Flanker task (requiring participants to respond to central stimuli while ignoring flanking distractions) has been widely utilized to detect cognitive control across the lifespan [9]. The conflict resolution cost (measured by performance decrements in incongruent compared to congruent conditions, e.g., slower reaction time) exhibits a U-shaped trajectory with age [10], reflecting an inverted U-shaped pattern in actual cognitive control efficiency, where higher cost indicates poorer control capacity. Similar results have been observed in other conflict tasks, such as the color-word Stroop (requiring participants to name the ink color of a word that is incongruent with the word's semantic meaning) [11]. Recent large-cohort studies have also found that gray and white matter volumes across all brain regions exhibit overall inverted U-shaped trajectories with age, with the gray matter volume peaking at early adolescence and the white matter volume peaking at young adulthood [12]. During late adulthood, normal ageing yields a protracted decline of brain structure, with the volumes of both gray matter and white matter reduced [8]. Consistently, the gray matter volumes of the frontal and parietal regions, which are essential in cognitive control tasks [13], have also been found to increase during early childhood and atrophy in early elderly age [14]. These findings are consistent with the view that cognitive control is a fluid intelligence, which reaches peak efficiency in young adulthood after progressive maturation since infancy, followed by age-related decline [4].

However, it remains largely unknown how brain activities related to cognitive control change over the lifespan. Previous research has primarily focused on brain activities in either youths or elderly adults, rather than examining changes across the entire lifespan, leaving the question of the lifespan cognitive control-related brain activities trajectory unclear. There is a possibility that the brain activities mirror the inverted U-shaped behavioral and anatomical developmental trajectories. However, no definitive conclusions can be drawn, as there are conflicting theories regarding their relationships. A naïve hypothesis about the brain-behavior relation is that higher cognitive control-related brain activities support better behavioral performance [15]; however, there is also evidence suggesting that better performance underlies more efficient (and thus lower) brain activities [16]. In terms of brain structure, synaptic pruning and myelination may enhance neural efficiency, potentially reducing blood oxygen level dependent (BOLD) signal in adulthood compared to adolescence, but the relationship between structural changes (e.g., synaptic density, gray/white matter) and functional development (BOLD signal) remains complex and inconsistently correlated across regions and tasks [17]. Furthermore, previous empirical studies regarding the brain activities across age have shown inconsistent findings. With conflict paradigms, children and adolescents are often found to have lower brain activities than young adults in frontoparietal regions [18]. However, brain activity differences in elderly adults as compared to young adults during cognitive control tasks have been less consistently reported [8]. Some studies have found that elderly adults have lower neural activities in frontoparietal regions than young adults [19], possibly because elderly adults may be unable to engage in an equal level of control-related activity due to functional decline. On the other hand, other studies have found that elderly adults may exhibit greater brain activities in frontoparietal regions than young adults (e.g., [20]), possibly because they have recruited additional brain regions to compensate for their decreased efficiency in utilizing control resources. Adding to the debate, it has been proposed that the cognitive control function in elderly adults might not decline at all [21]. These conflicting findings underscore the complexity of understanding age-related differences in cognitive control.

In addition to understanding the age-related change of individual brain region activation, previous research has also suggested that the overall distribution of brain activity changes with age. Two notable phenomena have emerged as significant findings in the field of aging research: compensatory recruitment of additional brain regions and a decrease in hemispheric asymmetry in brain activities. The concept of compensatory recruitment posits that, while aging may lead to reduced functionality in specific brain areas, older adults can mitigate this decline by engaging alternative neural circuits or regions. This compensatory mechanism serves as a form of neural adaptation to the challenges of aging, allowing for the preservation of cognitive function despite age-related physiological changes [22]. Similarly, some developmental studies have also reported compensatory brain recruitment in young children [23]. In parallel, previous studies have reported a decrease in hemispheric asymmetry in older populations. This phenomenon, often referred to as the hemispheric asymmetry reduction in older adults (HAROLD) model, proposes that older adults exhibit a reduced laterality of brain activation compared to younger individuals [24]. This phenomenon might reflect a form of neural compensation, where both hemispheres are utilized to perform tasks that once predominantly engaged only one hemisphere [25].

Few studies have directly tested the change of brain activities related to cognitive control across the lifespan. One existing study observed a positive association between the activation of the bilateral prefrontal cortex and age [26]. Given the relatively small sample size (n = 30), the reliability of these findings is somewhat limited. As a result, it is difficult to draw a clear conclusion about how brain activities related to cognitive control change across the entire age range.

One direct way to test the lifespan trajectory of brain activation related to cognitive control is to conduct a large cohort of neuroimaging studies with participants covering a wide age range. To the best of our knowledge, such studies have not yet been conducted. An alternative approach is to utilize meta-analyses to combine the results of existing studies targeting different age groups. Compared to the large cohort studies, meta-analyses are more accessible and resource-saving. In addition, meta-analyses can increase the statistical power and generalizability by combining various studies, reducing heterogeneity and bias from individual studies' methods, populations, or confounding variables [27]. Several neuroimaging meta-analyses have examined age-related changes of cognitive control-related brain activities [19,28,29], but limitations such as incomplete age coverage [19,28] and insufficient studies in certain age ranges [29] prevent them from appropriately answering questions about the lifespan trajectory of cognitive control functions. These studies have primarily focused on spatial convergence and/or diversity of coordinates across different age ranges, offering limited insights into lifespan trajectories of activity strength. Although a few studies have attempted parametric meta-regression to examine the age-related differences in cognitive control-related brain activities (e.g., [28]), they have been constrained by utilizing linear models that may overlook nonlinear trajectory patterns such as the inverted U-shaped trend.

The goal of this study is to provide a comprehensive examination to reveal the lifespan trajectory of brain activities responsible for cognitive control. Instead of encompassing various aspects of cognitive control, we focus on conflict processing for several rea-

sons. First, conflict processing reflects the fundamental cognitive control ability to maintain a goal while avoiding distractions [30]. Second, its mechanisms in young adults are relatively well-known, with the frontoparietal and cingulo-opercular networks engaged [13], providing a baseline reference for our study. Third, conflict tasks with neuroimaging data have been widely applied to both younger and older groups, making a systematic meta-analysis feasible. Lastly, different conflict tasks share key components of cognitive control [1], such as conflict monitoring and inhibitory control, which enable us to conduct effect-size-based meta-analyses using the congruency effect (i.e., the contrast between incongruent and congruent/neutral conditions). Including other sub-processes of cognitive control may introduce heterogeneity and make effect sizes incomparable.

In this study, we aim to address the question of the lifespan trajectory of cognitive control-related brain activities via a systematic meta-analysis. By analyzing age-related changes with multiple regression models in whole-brain analyses, we first demonstrate that the major detectable lifespan trajectory for cognitive control brain activity is inverted U-shaped. Subsequent generalized additive model (GAM) analyses refined this trajectory, revealing peak brain activity between 27 and 36 years of age. Notably, comparisons between a few simpler models revealed that the square root model best characterized these trajectories. Finally, we show that laterality changes as a U-shaped pattern across the lifespan.

2. Materials and methods

2.1. Literature preparation

2.1.1. Literature search

We report how we determined all data exclusions (if any), all manipulations, and all measures in the study. We first searched both English and Chinese articles on the youth and the elderly from PUBMED, Web of Science, and CNKI (China National Knowledge Infrastructure) till April 30, 2025. The following search terms were applied in titles, abstracts, table of contents, indexing, and key concepts: (*"Stroop" OR "Flanker" OR "Simon" OR "SNARC" OR "Navon" OR "interference" OR "cognitive conflict") AND ("fMRI" OR "functional resonance imaging" OR "functional imaging" OR "neuroimaging" OR "PET") AND ("children" OR "kids" OR "adolescents" OR "teenagers" OR "underage" OR "aged" OR "old" OR "older" OR "elder" OR "elderly" OR "senior" OR "development" OR "developmental" OR "aging" OR "life span"*). The above process yielded 5112 articles. In addition, 111 studies on young to middle-aged adults were included in the literature pool from a previous meta-analysis study [13], where an additional 40 studies were excluded according to the current literature exclusion criteria (see below). Moreover, we screened 16 articles citing or being cited by the crucial literature (influential review articles or meta-analyses in the field, typically with over 500 citations). After removing duplicates, the literature search identified 4213 articles.

2.1.2. Exclusion criteria

We excluded any articles that met one or more of the following predefined exclusion criteria: (1) not in English or Chinese; (2) not including healthy human participants; (3) case study; (4) not empirical study; (5) not functional resonance imaging (fMRI) or positron emission tomography (PET) study; (6) not whole-brain results (i.e., not have covered the whole gray matter); (7) not in Talairach or Montreal Neurological Institute (MNI) space; (8) not reflecting the congruency effect (i.e., contrasts between incongruent and congruent or between incongruent and neutral conditions); (9) not reporting the exact mean age of participants.

A total of 125 articles with 139 studies were identified as eligible for inclusion in our meta-analyses. No statistical methods were used to pre-determine sample sizes, but our sample sizes are similar to or larger than those reported in previous publications [19,31]. Fig. S1 (online) shows the preferred reporting items for systematic reviews and meta-analyses [32] flow chart for the literature screening process. The detailed description of the features for included studies is available in Text S1 and Table S1 (online).

2.2. Coding procedure

A coding manual was formulated to record pertinent study information, including authors, publication dates, experimental tasks, contrasts, and sample demographics (such as the average age and sample size). To ensure coding accuracy, two authors independently coded all studies, with discrepancies resolved through discussion or reference to the original studies. In instances where studies lacked essential information, such as peak coordinates for relevant contrasts, participant age averages, or data for specific age groups, efforts were made to contact the authors via E-mail to obtain the relevant data. In addition, both coordinates and effect sizes (i.e., Hedge's g) were extracted from each study. Further, Talairach space coordinates were transformed to MNI coordinates using the Lancaster transform [33].

2.3. Meta-analytic procedure

2.3.1. Spatial convergence using activation likelihood estimation (ALE)

In order to obtain a comprehensive understanding of cognitive control-related brain activities across all age groups and to replicate a prior study [13], we initially conducted a single dataset meta-analysis using BrainMap GingerALE software [34] (version 3.0.2, http://www.brainmap.org). This meta-analytical approach, known as activation likelihood estimation, utilizes the spatial convergence of brain activity across multiple studies to determine the probability of activation in specific regions. Foci from individual studies were transformed into a standardized coordinate space and modeled as Gaussian probability values that accounted for variability in the number of participants in each study. In situations where foci overlapped across studies, multiple Gaussians were associated with a single focus, and ALE selected the Gaussian with maximum probability for each focus [34]. Subsequently, ALE score maps were generated by comparing these modeled Gaussian distributions with a null distribution that simulated random brain effects. The null distribution was generated using the same sample size and number of foci groups as the experimental dataset 1000 times. ALE scores were then used to calculate P values, which were based on the proportion of values higher than a certain threshold in the null distribution. This resulted in a statistical ALE map that differentiated true brain effects from random effects. A voxel-level cluster-forming threshold of $P < 0.001$ and a cluster-level family-wise error (FWE)-corrected threshold of $P < 0.05$ were utilized to compute ALE maps [35]. The thresholded brain map, initially in volumetric space, was subsequently projected onto the cortical surface using Surf Ice software (https://www.nitrc.org/projects/surfice). All surface-based visualizations presented in this study were generated using this method.

2.3.2. Spatial convergence using seed-based d (effect size) mapping (SDM)

SDM is an alternative approach to statistically synthesize results from multiple neuroimaging experiments. Similar to ALE, SDM employs a coordinate-based random-effect approach to amalgamate peak coordinate information into a standard space across

several experiments. However, while ALE solely considers the binary feature (i.e., active vs. inactive) of peak coordinates, SDM takes into account the quantitative effect size (can be positive or negative) connected to each peak and reconstructs the initial parametric maps of individual experiments before amalgamating them into a meta-analytic map [36]. A previous study [37] suggested that the SDM exhibits superior sensitivity compared to traditional coordinate-based meta-analytical approaches, such as ALE. Therefore, the use of a distinct algorithm in SDM from ALE allows us to scrutinize the robustness and replicability of the outcomes obtained via ALE. More importantly, SDM enables the inclusion of covariates in the meta-regression analyses to reflect the changes in brain function across the lifespan.

We estimated the mean activation across all age groups using the software of SDM with permutation of subject images (SDM-PSI) (version 6.22, https://www.sdmproject.com). This analysis aimed to characterize the activation distributions of cognitive control-related brain regions across all studies, which was conducted utilizing the "Mean" function in the SDM-PSI software. Effect size maps were built for the 139 individual experiments. This was accomplished by (1) converting the statistical value of each peak coordinate into an estimate of effect size (Hedge's g) using standard formulas [38] and (2) convolving these peaks with a fully anisotropic unnormalized Gaussian kernel (α = 1, FWHM = 20 mm) within the boundaries of a gray matter template (voxel size = $2 \times 2 \times 2$ mm^3). Imputation (50 times) was conducted for each study separately to obtain a reliable estimate of brain activation maps [36,37]. In addition, the individual effect size maps were combined using a random-effect general linear model. To assess the statistical significance of activations in the resulting meta-analytic effect size map, 1000 random permutations of activation peaks within the gray matter template were compared. Finally, the meta-analytic maps were thresholded using a voxel-wise FWE corrected threshold of $P < 0.001$ and a cluster-wise extent threshold of 100 voxels [39,40]. This approach is in line with the recent methodological recommendations advocating for more stringent statistical criteria in neuroimaging meta-analyses, aimed at improving reproducibility (e.g., [41]).

Results from this analysis were further used as regions of interest (ROIs) in the subsequent model fitting analyses (see section "2.3.5 *GAM fitting*" below). The possibility of publication bias for resultant clusters was examined using Egger's test, in which any result showing $P < 0.05$ was regarded as having significant publication bias. Heterogeneity was evaluated using the I^2 index, which quantifies the proportion of total variability attributable to heterogeneity between studies. A value less than 25% indicates low heterogeneity among the included studies [42].

2.3.3. Detecting different trajectories with contrast analyses

To test how cognitive control-related brain activities change with age, we categorized each study based on the mean age of participants into youth (<18 years), young to middle-aged adults (18 –59 years), and elderly (≥60 years) groups. The age boundaries were determined to minimize age distribution overlap. We utilized SDM-PSI to perform a contrast analysis between the group of young to middle-aged adults and the combination of other groups in order to examine whether there are brain regions that exhibit an inverted U-shaped lifespan trajectory. This was achieved by assigning studies from the young to middle-aged adult group as 1 and all other studies as −1 in the "linear model" function of SPM-PSI. This analysis yielded two results: one showing higher activity in young to middle-aged adults than the youth and elderly groups, and the other showing the opposite. Like the mean analysis, results from this analysis were used as ROIs in the subsequent model fitting analyses (see sections "2.3.5 *GAM fitting*" and "2.3.6 *Model simplification and model comparison*").

In addition, to explore other possible trajectories, such as the increase-and-stable pattern [4], we conducted contrast analyses between the youth and the combined group of young to middle-aged and the elderly, as well as between the elderly and the combined group of youth and young to middle-aged adults. Furthermore, to address the controversies in previous studies (e.g., [19,20]), we conducted contrast analyses between elderly and young to middle-aged adult groups; for comprehensive lifespan coverage, we likewise performed contrast analyses between the youth and young to middle-aged adult groups.

2.3.4. Data extraction

Masks were generated for each ROI derived from the mean and contrast analyses in SDM-PSI as described above. For contrast analyses, entire activated regions were treated as single ROIs. However, given that mean analyses revealed disproportionately large clusters, we abandoned whole-ROI usage and instead constructed sphere ROIs: each was a spherical ROI centered on the peak coordinate with a 4-voxel radius (approximately 257 voxels in total, generated via AFNI's *3dUndump -srad 4*). Subsequently, we extracted the effect sizes for each mask. For studies lacking activation reports in specific meta-analytic regions, effect sizes were imputed as non-significant values bounded by each study's statistical threshold, following SDM-PSI's multiple imputation protocol [37]. One value was obtained from each of the fifty SDM imputations and subsequently averaged for each study in each region. The iterated variances were also averaged in a similar way. Additionally, we removed the outliers (beyond 3 standard deviations from the mean) in the following model fitting analyses.

2.3.5. GAM fitting

To precisely estimate the inverted U-shaped trajectories, we adopted the GAM to fit the curves. The GAM allows for flexible, nonparametric smoothing of predictor variables [43] and has been widely used to depict the lifespan trajectories (e.g., [12]). We implemented GAMs using the "mgcv" package [43] in R, employing the default basis dimension (k = 10) for smooth terms. For each ROI, we fitted a GAM with the formula (1) below:

$$g \sim s(age) + covariates, \quad (1)$$

where g is the effect size (dependent variable), s(*age*) represents a smoothing spline of age (predictor variable), and *covariates* represent the dummy-coded categorical covariate regressors. These regressors correspond to eight aspects of the included studies: (1) the presence of various conflict types (e.g., Stroop or Simon), (2) the mixed subject samples based on handedness (e.g., right handed only or both handed), (3) the different contrasts in reporting congruency effects (e.g., incongruent – congruent or incongruent – neutral), (4) different trial types regarding whether they excluded error trials, (5) the use of different types of experimental design (i.e., event-related or block designs), (6) the behavioral congruency effects measured by reaction time, (7) the sample sizes, and (8) the gender ratios defined by the proportions of female participants. Notably, we adopted median imputation for 9 studies (accounting for 6.98% of the total included studies) not reporting the behavioral congruency effects, and included an indicator regressor to account for the potential impact of imputation. The validity of this imputation approach was confirmed through a robustness analysis (Text S6 online). We incorporated these covariates to control for their potential confounding effects related to age, which could otherwise influence our results. We also adjusted the estimate with a weight parameter, which was the reciprocal of variance. We used penalized regression splines, with the amount of smoothing determined automatically based on generalized cross validation. The resulting P values were false discovery rate (FDR) corrected.

For each ROI, we quantified the peak age by choosing the highest prediction of a fine-grained age scale (1000 points from 8 to 74 years old). We also calculated the estimated degree of freedom for the smooth curve by summing up the degree of freedom for each penalized term (i.e., s(*age*).1 to s(*age*).9). Additionally, we quantified the contribution of age by computing the difference in adjusted R^2 between the full model (including the s(*age*) term) and a deprecated model (excluding s(*age*)), with the resulting value representing the variance uniquely explained by age-related effects after accounting for other covariates in the model.

2.3.6. Model simplification and model comparison

While the GAM analysis may yield good fitting results on the data, it is important to acknowledge its potential limitations. One concern is that it can fit the data with high degrees of freedom (up to 5.0, Table S4 online), which makes it susceptible to overfitting and harder to generalize. Another issue is its poor interpretability. Therefore, we next sought to fit the data with simpler models.

To this end, we used the "metafor" package in R to fit these effect sizes with the age and its derivatives as predictors. Specifically, we tested four non-linear models (see formulas (2)–(5) below). Quadratic and cubic models were included based on previous studies (e.g., [44]); quadratic logarithmic and square root models were included to capture the possible skewed trajectory, which would reflect the asymmetric trajectory of development and decline of cognitive control [4]. Each model was fitted to each ROI separately. In addition, we included the same covariates as the GAM analysis in each regression model. We calculated the Akaike information criterion (AIC) to evaluate the goodness of fit for each model. Note that model comparison does not include the GAM due to fundamental differences in model structure and likelihood function, which make their AIC values not directly comparable.

i: Quadratic model

$$g \sim age + age^2 + covariates, \tag{2}$$

ii: Cubic model

$$g \sim age + age^2 + age^3 + covariates, \tag{3}$$

iii: Quadratic logarithmic model

$$g \sim \log(age) + (\log(age))^2 + covariates, \tag{4}$$

iv: Square root model

$$g \sim age + \mathrm{sqrt}(age) + covariates. \tag{5}$$

2.3.7. Fitting square root and linear trajectories with whole-brain meta-regression analyses

To better describe the possible lifespan trajectories of the whole brain, we carried out meta-regression analyses with the age and/or its derivatives as regressors using the SDM-PSI software. The preprocessing was the same as the mean analysis described above. Two regressions were conducted across the whole-brain, including a linear regression (with only age as the regressor) and a square root regression (with age and its square root as separate regressors). The linear regression aimed to test regions with increasing/decreasing activity with age, and the square root regression aimed to test regions with the inverted U-shaped trajectories based on the model fitting analyses (see section "3.5 Model simplification of the lifespan trajectories").

2.3.8. Laterality analysis

We calculated the laterality based on the effect sizes of reported brain coordinates from each study. We computed the sum of effect sizes across coordinates for the left and right hemisphere, respectively, yielding one global effect size each (i.e., g_L and g_R). Then, we calculated the index of brain laterality [45] with the formula (6):

$$laterality = \frac{g_L - g_R}{g_L + g_R}, \tag{6}$$

which was then submitted to the GAM and simplified models (i.e., the quadratic, cubic, square root, and quadratic logarithmic models).

3. Results

3.1. Sample description

A total of 5239 articles were identified, including 5112 articles searched from the database, 111 articles adopted from a previous study [13], and 16 articles searched from the references of crucial articles. After excluding duplicates and applying exclusion criteria, 125 articles including 139 studies with 3765 participants and 1685 brain activation foci, were included in this meta-analytic study (Fig. S1 and Table S1 online). The average age of participants ranged from 8 to 74 years, with the individual age ranging from 5 to 85 years. A demonstration of the age distribution for each included study is presented in Fig. S2 (online).

3.2. Regions related to cognitive control identified by SDM

We calculated the average brain activation based on the effect sizes reported in all studies using the SDM-PSI software. We found significant activation in the frontoparietal regions (left inferior parietal lobule, right inferior frontal gyrus, and right middle frontal gyrus, MFG), the cingulo-opercular regions (left anterior cingulate cortex), and other regions including bilateral inferior temporal gyrus (ITG) (Fig. 1 and Table S3 online). In addition, a robustness analysis suggested that controlling for age as a covariate did not alter the spatial distribution of mean activation patterns in the SDM analysis (Fig. S3 and Table S3 online). Furthermore, to enhance the replicability and robustness of our findings and enable

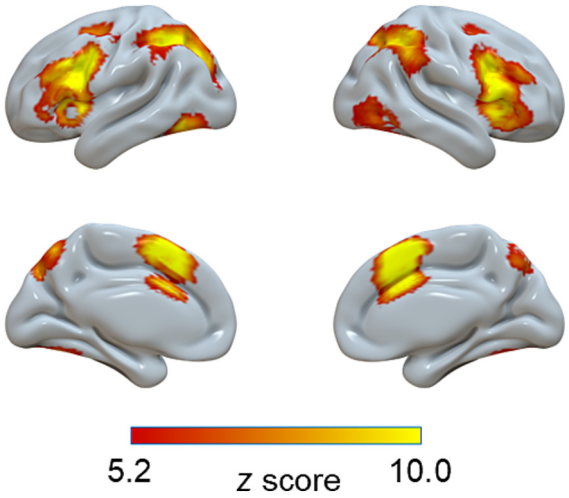

Fig. 1. Regions identified from the mean analysis in SDM. The results revealed significant activation in the frontoparietal regions (left inferior parietal lobule, right inferior frontal gyrus, and right middle frontal gyrus), the cingulo-opercular regions (left anterior cingulate cortex), and other regions including bilateral inferior temporal gyrus. The meta-analytic maps were thresholded using a voxel-level family-wise error (FWE) corrected threshold of $P < 0.001$ and a cluster-wise extent threshold of 100 voxels.

direct comparison with a previous study [13], we also conducted the mean analysis across all studies with the ALE. The detailed results are shown in Text S2, Fig. S4, and Table S2 (online).

3.3. Trajectories of cognitive control regions identified in the mean analysis

Having identified six brain regions in the mean analysis using SDM-PSI, we proceeded to explore how the activation levels of these regions change with age. To this end, we extracted brain activity data from all studies for each identified region. Given the large cluster size of some regions (up to 10,000 voxels), we used round brain masks centered at each peak coordinate and extending 4 voxels. Before performing the meta-regression, we verified the effectiveness of using mean age as a predictor with a simulation approach (Text S3 and Fig. S5 online). We then subjected the extracted data to separate GAM analyses, factoring in the confounding covariates (see section "2.3.5 *GAM fitting*"). The analyses (Table S4 online) revealed significant age-related changes in the activation levels of 2 out of the 6 regions (Fig. 2, l-ITG and r-MFG), *P*-FDR < 0.05. Visualization of the trajectories suggests that these regions showed inverted U-shaped patterns. The significance of their inverted U-shaped trajectories was further examined using a two-line test approach (Text S4 online). Results suggest that both regions involve an increase in activity from childhood to young adulthood (approximately up to 30 years of age), and one of them (l-ITG) showed consistent decrease in the later stages of age (Text S4 online). The other regions showed no significant age-related changes. Notably, none of the regions showed significant publication bias based on Egger's test (*p*s > 0.80), and they all showed low (to slightly moderate) between-study heterogeneity (τs < 0.14, *Q*s < 11.87, I^2s < 27.3%). This indicates that the observed results are not likely influenced by biased reporting or substantial variability in the included studies. A robustness analysis further ruled out the potential influence of including unpublished and non-English studies in this study (Text S6 and Fig. S6 online).

The peak coordinates may not fully represent cognitive control regions because they are sparsely distributed. We next use whole-brain analyses to estimate the lifespan trajectories.

3.4. Detecting different trajectories of whole brain activities

To explore various possibilities of lifespan trajectories, we grouped studies by their mean age into the youth, young to middle-aged adults, and elderly groups, and then conducted several contrast analyses (see section "2.3.3 *Detecting different trajectories with contrast analyses*"). These analyses did not reveal any regions that exhibited significantly higher or lower brain activity in the youth compared to others (the combination of young to middle-aged and older adults) (Table 1). Similarly, we did not observe any regions with higher or lower brain activity in older adults compared to others (the combination of the youth and young to middle-aged adults) (Table 1). These results excluded the possibilities of increase/decrease-then-stable and stable-then-increase/decrease trajectories (Fig. 3, panels d, f, g, and i). In addition, we failed to observe any region showing lower activity in young to middle-aged adults than others (the combination of the youth and elderly), and thereby ruled out the possibility of the upright U-shaped trajectory (Table 1, Fig. 3e).

However, we identified greater activity in young to middle-aged adults compared to others in the frontoparietal regions, including bilateral inferior frontal gyrus and bilateral inferior parietal lobule;

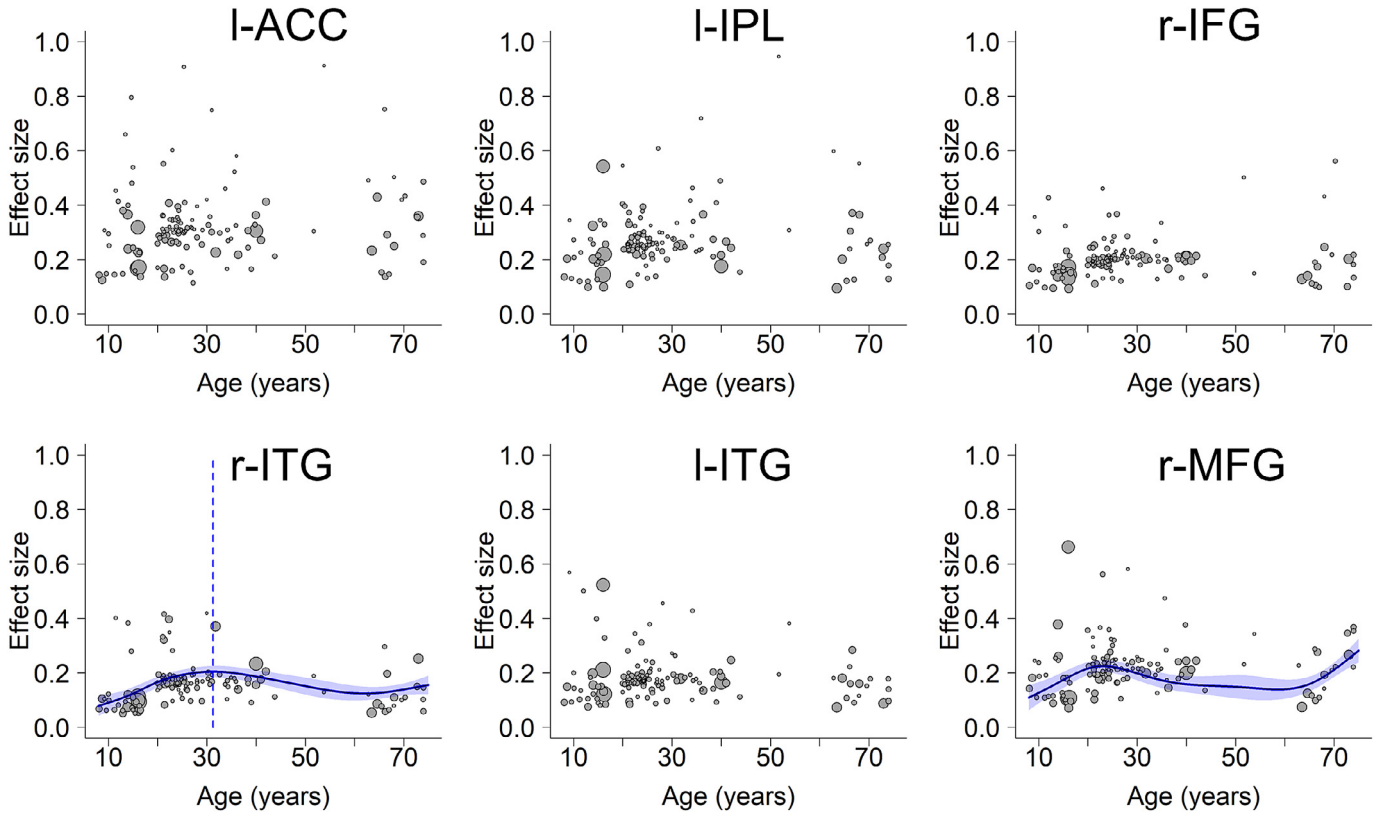

Fig. 2. Scatter plots of data extracted from peak areas identified based on the mean SDM analysis. The sizes of the scattered dots show the square root of model weights (1/variance) for each study. r: right; l: left; ACC: anterior cingulate cortex; IPL: inferior parietal lobule; IFG: inferior frontal gyrus; ITG: inferior temporal gyrus; MFG: middle frontal gyrus.

Table 1
Brain areas activated in the contrast of one age group versus others (voxel-wise FWE-corrected, $P < 0.001$, with minimum cluster size ≥ 100 voxels) with the SDM-PSI.

Order	# Voxels	Z	P	L/R	MNI coordinate			Anatomical location	BA
					x	y	z		
Young to middle-aged adults > Others									
1	1773	4.65	<0.001	R	50	12	2	Inferior frontal gyrus	48
2	919	4.42	<0.001	R	52	−46	38	Inferior parietal lobule	40
3	723	3.83	<0.001	/	0	−4	56	Supplementary motor area	6
4	610	4.17	<0.001	L	−44	14	26	Inferior frontal gyrus	48
5	301	3.87	<0.001	L	−34	−50	42	Inferior parietal lobule	40
6	167	3.80	<0.001	R	52	−62	2	Middle temporal gyrus	37
7	133	3.07	<0.001	L	−38	24	−2	Insula	47
Young to middle-aged adults < Others									
None									
The youth > Others									
None									
The youth < Others									
None									
The elderly > Others									
None									
The elderly < Others									
None									

Note: the brain regions in the table correspond to the regions in Fig. 4. MNI: montreal neurological institute; BA: brodmann area; L: left; R: right.

the cingulo-opercular regions, including supplementary motor area and left insula; and other regions, including the left middle temporal gyrus (Fig. 4 and Table 1). This result essentially supports an inverted U-shaped trajectory. Notably, none of the clusters showed significant publication bias based on Egger's test (*P*s > 0.70), and they all showed low between-study heterogeneity (τs < 0.12, *Q*s < 11.13, I^2s < 21%). This indicates that the observed results are not likely influenced by biased reporting or substantial variability in the included studies. Consistently, further contrast analyses revealed that the young to middle-aged adults showed greater activity than both the youth (Fig. S7 and Table S8 online) and the elderly (Fig. S10 and Table S8 online).

3.5. Fitting the lifespan trajectories with the GAM

For each region identified from the contrast between young to middle-aged adults and others, the GAM could fit the data significantly with a smooth curve (Fig. 4), with degrees of freedom varying from 3.6 to 5.0. Peak ages of the inverted U-shaped trajectories were between 27.7 and 35.7 years. Detailed statistics are shown in Table S4 (online).

3.6. Model simplification of the lifespan trajectories

Considering the GAM may overfit the data, we fitted the results with simpler models commonly adopted in lifespan developmental literature (e.g., [44]), including the quadratic and cubic functions, as well as less common models, including square root and quadratic logarithmic functions, and estimated the goodness of fit by comparing their AIC (see section "2.3.6 *Model simplification and model comparison*"). Results showed that the square root model demonstrated the best goodness of fit for all these regions (Table S5 online). We also calculated the peak age for each region based on the square root model, and the results showed that the peak ages ranged from 32.6 to 35.0 years (Fig. 4 and Table S6 online).

3.7. Fitting the whole brain with square root and linear models

Based on model comparisons, we found that the square root model provided the best goodness of fit for the age-related change of the brain activities. To supplement the inverted U-shaped results from the contrast analysis, the square root function was then submitted to whole-brain meta-regression analyses in SDM-PSI (see section "2.3.7 *Fitting square root and linear trajectories with whole-brain meta-regression analyses*").

By fitting the activation over the whole brain, we found six significant brain regions, including the bilateral inferior frontal gyrus, bilateral inferior parietal lobule, supplementary motor area, and middle temporal gyrus (Fig. S9a and Table S7 online). These results further supported the existence of the inverted U-shaped regions we initially identified (Fig. 4).

In addition, we explored the whole-brain trajectories with a linear meta-regression (see section "2.3.7 *Fitting square root and linear trajectories with whole-brain meta-regression analyses*"). However, no significant regions were observed (Fig. S9b online).

3.8. Lifespan trajectories of the laterality

We also tested how the laterality of the brain activity changes with age (see section "2.3.8 *Laterality analysis*"). We first modeled the laterality trajectory using the GAM. Results showed a significant age effect, $F(2.5, 3.1) = 2.99$, $P = 0.033$, $R^2 = 0.06$. Moreover, we fitted the data with the four simplified models (i.e., the quadratic, cubic, square root, and quadratic logarithmic models). The results showed that a square root function provided the best goodness of fit, with the $\beta_{sqrt(age)} = -0.65$ (95% CI = [−1.04, −0.26]), $P = 0.001$. The two-line test suggests the hypothetical peaks from both models did not reach significance (Text S4 online). A visually upright U-shaped trajectory indicated that the youth and elderly adults tended to be more left-lateralized across the whole brain (Fig. S12 online). A further comparison of the relative levels of laterality across different age groups revealed that both the youth and the elderly groups exhibited greater left lateralization than the young to middle-aged adult group (Text S5 online).

4. Discussion and conclusion

The present study yielded two primary findings: (1) Among different possible trajectories, only the inverted U-shaped trajectories were reliably observed in the whole-brain analyses, with GAM analyses revealing peak activation between 27 and 36 years; comparisons among simpler models suggested that the square root function provided the optimal characterization of these trajectories; (2) The youth and the elderly demonstrate weaker brain activities and a relatively greater extent of left laterality compared to

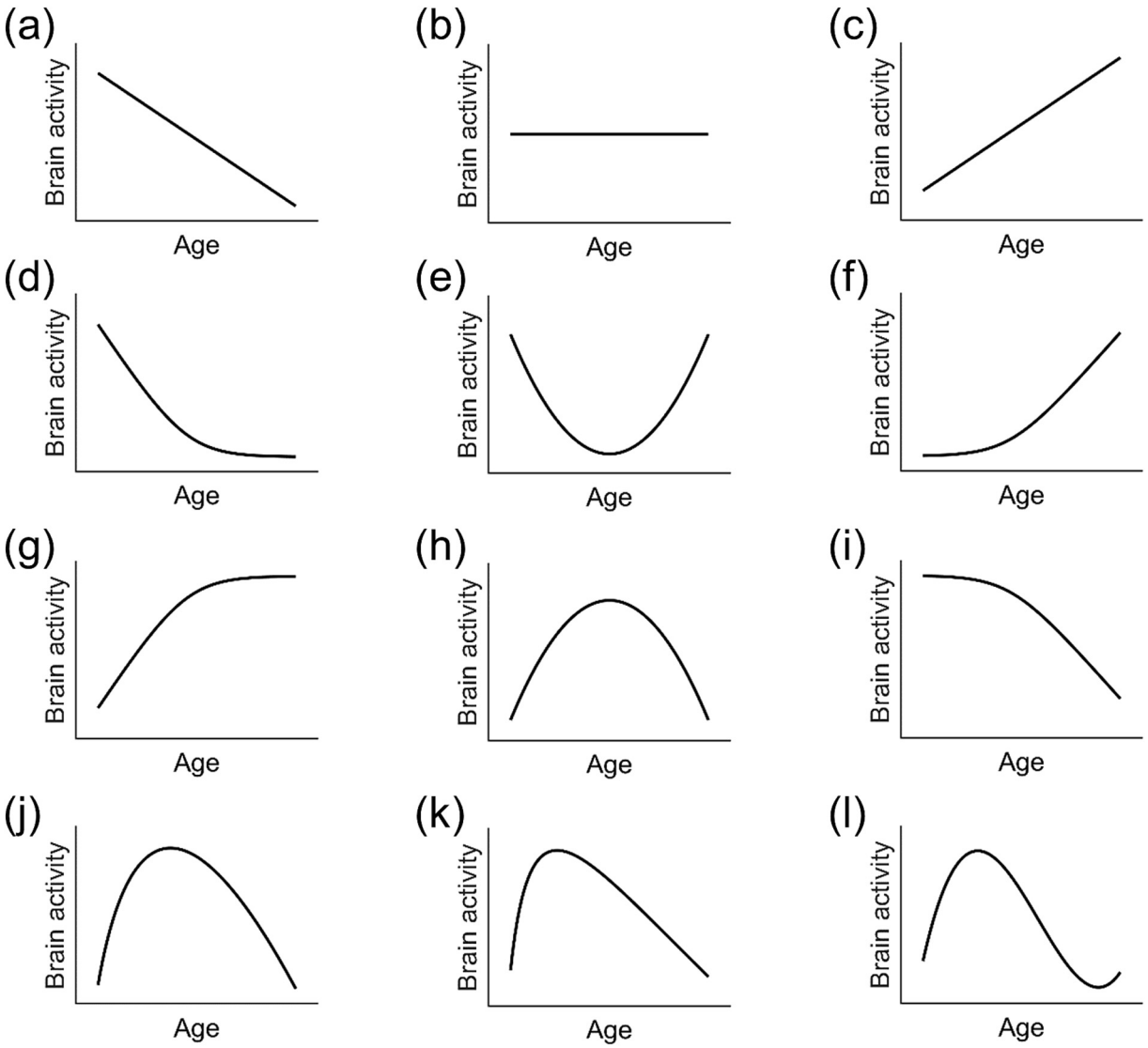

Fig. 3. The lifespan trajectories explored in our study. Panels (a–c) show linear decrease, flat, and linear increase patterns, respectively, and were modelled with the linear function. Panels (e) and (h) show the upright and inverted U-shapes, respectively, and were tested with the contrast between young to middle-aged adults and others, as well as with the quadratic function. Panels (d, f, g, i) show combinations of a stable period and an increase/decrease period across the lifespan, and were tested with the contrast between the youth and others, or between the elderly and others. Panels (j, k, l) show the variants of inverted U-shaped trajectories, which capture the possibly early peak feature. They were tested with square root, quadratic logarithmic, and cubic functions, respectively.

the young to middle-aged adults. These results provide strong evidence for the existence of cognitive control regions exhibiting inverted U-shaped trajectories.

4.1. The Inverted U-shaped trajectory of brain activity related to cognitive control

The main finding is that a wide range of cognitive control regions follow inverted U-shaped lifespan trajectories, but no regions showed decrease-then-stable (Fig. 3d), upright U-shaped (Fig. 3e), stable-then-increase (Fig. 3f), increase-then-stable (Fig. 3g), stable-then-decrease (Fig. 3i), or linear trajectories (Fig. 3a and c).

The greater activation in the frontoparietal control network among young to middle-aged adults compared to the youth and the elderly supports the notion that cognitive control abilities may not be fully developed in children and may decline in the elderly. This finding is consistent with the idea that the cognitive control system is most effective in young adulthood, suggesting a possible correlation between the higher functional activations in the brain and the superior performance of young adults on cognitive control tasks [46]. Consistently, a previous study [47] showed that behavioral performance (success of interference suppression) is positively correlated with the activity in frontal regions.

The inverted U-shaped trajectory of brain activation might be associated with the development of brain structure and functional changes. First, it may reflect the well-documented structural changes that occur in these regions across the lifespan, which include synaptic pruning, myelination, cortical thinning, and white matter maturation [12]. For example, the density of dopamine receptors increases during adolescence and young adulthood and subsequently declines with age [48], affecting neurotransmitter bioavailability that supports functional differentiation of neural networks. These changes may affect the efficiency and connectivity of neural circuits within the frontoparietal control network [49]. Second, the inverted U-shaped trajectory may also arise from functional changes resulting from the modulation of neurotransmitters, hormones, and environmental factors [50]. As suggested by lifes-

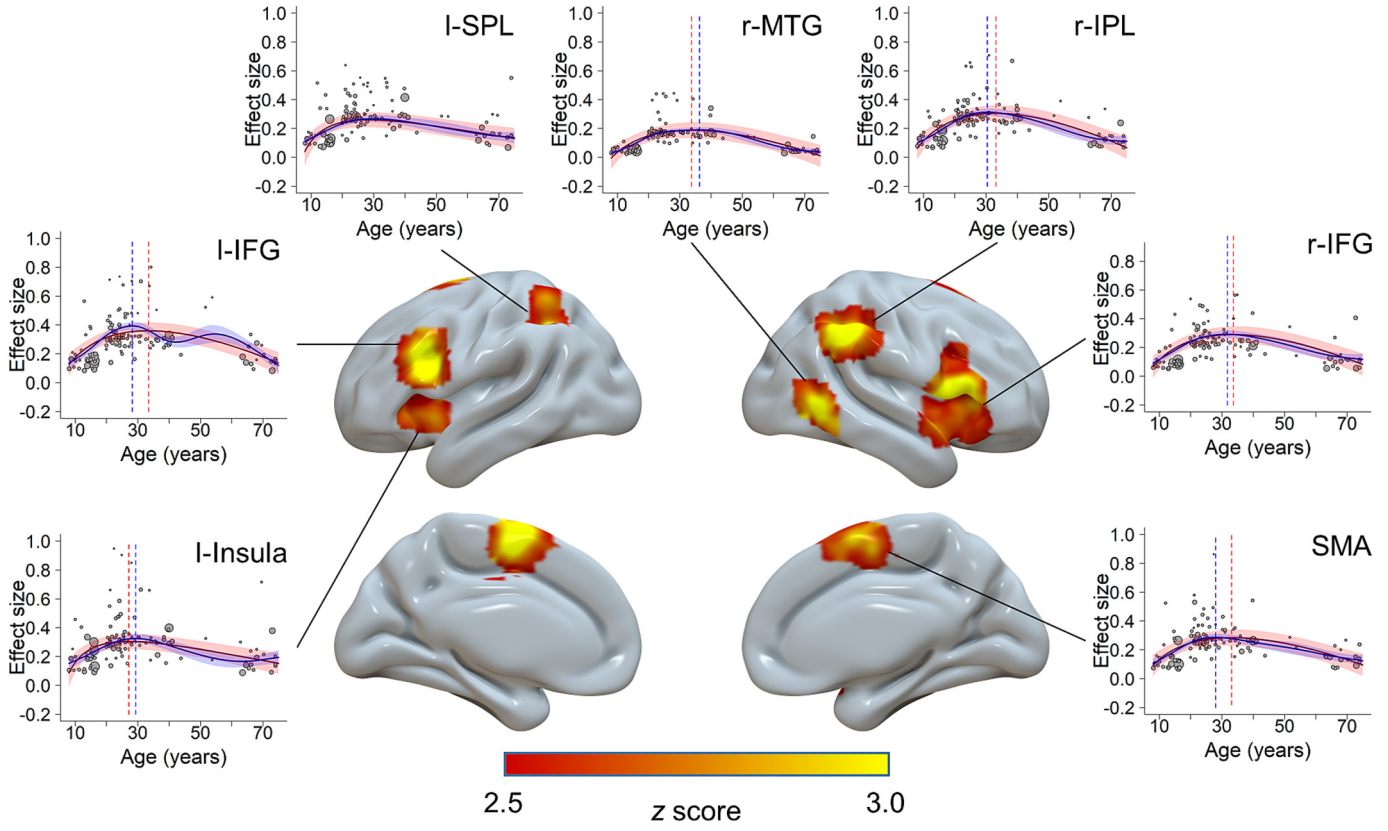

Fig. 4. Brain regions showing inverted U-shaped trajectory patterns. Scattered plots are the effect size as a function of age, with curves fitted by GAM (blue color) and the best simplified model (red color). Shaded areas around the curves represent standard errors. Dashed vertical lines show peak ages estimated from GAM (blue) and simplified model (red). The sizes of the scattered dots show the square root of model weights (1/variance) for each study. The brain maps were thresholded using a voxel-level family-wise error (FWE) corrected threshold of $P < 0.001$ and a cluster-wise extent threshold of 100 voxels. r: right; l: left; IFG: inferior frontal gyrus; SPL: superior parietal lobule; MTG: middle temporal gyrus; IPL: inferior parietal lobule; SMA: supplementary motor area.

pan studies, optimal neurotransmitter bioavailability facilitates higher-fidelity regional activation patterns, which may contribute to the observed trajectory [51,52]. Understanding change patterns of brain structure and function is critical for developing interventions and treatments aimed at improving cognitive control abilities across the lifespan.

4.2. Implications for the compensatory and asymmetry reduction theories

Critically, there was no region showing higher activity in the elderly compared to the young to middle-aged adults, but we observed several regions showing the opposite (Text S5 and Table S8 online). The results persisted after we controlled the behavioral congruency effect (Text S6 and Fig. S11 online), thereby ruling out the possibility of weaker brain activity associated with poor behavioral performance in the elderly. The observed decrease in brain activation among the elderly might be attributed to several interrelated factors. First, cognitive control regions, especially the frontal area, tend to shrink with age, leading to a reduction in overall brain volume and potential loss of synaptic integrity [53]. This shrinkage can impair the brain's ability to effectively process and manage complex tasks. Another significant factor is the impairment of neurovascular coupling, the relationship between neuronal activity, synaptic function, and subsequent blood flow, which disrupts the brain's ability to maintain optimal function during cognitive tasks [54]. Furthermore, the decrease in cerebral blood flow with age can diminish the delivery of essential nutrients and oxygen to the brain, impairing its overall functionality [55]. These changes could lead to regional abnormalities, such as blood flow, blood volume, metabolic rate, or BOLD-derived physiologic proxies like the fractional amplitude of low-frequency fluctuation and regional homogeneity [56]. Future studies may validate and extend our study by adopting the age-sensitive regions we observed and testing other measurements, such as resting-state data, which are more easily collected in large-scale studies involving children and the elderly compared to task-based activations.

The compensatory theory [22] proposes that the elderly recruit additional brain regions to compensate for age-related cognitive decline, but our results did not show this pattern. We suggest that the absence of compensatory upregulation in frontoparietal regions among the elderly observed in our study might be attributed to limited available resources when cognitive control-related brain regions are already fully engaged [57]. Previous research has shown that younger adults recruit lower activity in frontoparietal regions during the congruent condition but significantly greater activities during the incongruent condition. In contrast, older adults already show a relatively higher activation during the congruent condition, leaving limited capacity for further increases in activation during the incongruent condition [58]. This is consistent with our findings, which are based on the contrast between incongruent and congruent conditions. Moreover, the nature of the task investigated might influence whether there is an upregulation in cognitive control regions with age. Upregulation in the frontal regions usually compensates for memory and sensory declination due to deficits in the hippocampus and sensory cortices [25]. Semantic cognition [45] might also be a target of compensation. However, conflict tasks seem to rely minimally on memory,

and involve relatively simple sensory stimuli (e.g., colors and locations) and simple semantic processing (e.g., reading a word). As such, conflict tasks may not necessitate compensation in these functions.

In addition, compensation in older adults may manifest as increased recruitment of bilateral regions and homologues with age [22]. The HAROLD theory [24] suggests that older adults typically exhibit less lateralization, either as a compensatory response to functional deficits or as a reflection of neural dedifferentiation. However, we observed that the elderly showed greater left lateralization compared to young to middle-aged adults. This may suggest that neural resources in the right hemisphere are more limited in the elderly, reducing their capacity to compensate for cognitive demands. This notion aligns with prior research indicating that functional connectivity within the frontoparietal control network is more disrupted in the right hemisphere than in the left during ageing [59]. Stronger patterns of left laterality were also identified in childhood in the current study, primarily noticeable within the prefrontal region, which may reflect the earlier development of the left hemisphere compared to the right [60]. Interestingly, our analyses revealed that young adults exhibited the lowest lateralization across the lifespan, contrasting with previous studies that reported stronger laterality in young adults. This discrepancy may stem from the small sample sizes and non-quantitative methods used in previous studies to calculate laterality [61]. Moreover, the laterality findings might be misinterpreted if the laterality hemisphere is disregarded, as both left and right lateralized results have been observed.

4.3. Conclusion

Our meta-analysis adopted advanced meta-regression approaches to chart the lifespan trajectories of cognitive control-related brain activities. The predominant lifespan trajectory is inverted U-shaped, peaking between 27 and 36 years. No other trajectory patterns were observed, highlighting the predominance of the inverted U-shaped pattern in the lifespan trajectory of cognitive control. Furthermore, we found that the youth and elderly showed a more asymmetric brain distribution than young to middle-aged adults. In sum, these results demonstrate the systematic age-related changes in cognitive control brain function.

4.4. Limitations of the results

One caveat to consider in this study is the non-uniform distribution of age among the included studies. Specifically, there is a noticeable gap in the age range of 45 to 60 years. Consequently, the observed age distribution could potentially influence the results of the regression analysis. We hope that future research could allocate more attention to the middle-aged period, considering the significant cognitive and neural changes during this stage, such as the onset of cognitive decline [9]. Nevertheless, it is worth noting that previous studies have indicated that the behavioral performance [62] and frontoparietal brain activations during conflict processing [63] in middle-aged individuals typically fall between those of younger and older adults. Furthermore, large cohort studies (e.g., [10]) often depict a smooth trajectory across these age groups. Therefore, we believe it is reasonable to consider the potential data from middle-aged individuals as part of the continuum in the lifespan trajectory.

Another notable limitation is that the available behavioral data cannot support robust analyses to address questions regarding behavioral lifespan trajectories, due to several reasons (Text S7 and Fig. S13 online). Given that the major focus of our current study is the brain activity, we exercise caution in overinterpreting the behavioral results.

In addition, it is crucial to avoid the occurrence of ecological fallacy (associations observed at the group level are erroneously assumed to apply to individuals) when interpreting the results of meta-regression analyses. Therefore, associations between brain activities and age across various studies do not provide direct insights into the specific age-related changes at the individual level. Future research incorporating individual-level investigations (e.g., longitudinal follow-up studies) is crucial to obtaining a more comprehensive understanding of these relationships.

Conflict of interest

The authors declare that they have no conflict of interest.

Acknowledgments

This work was supported by the National Natural Science Foundation of China (NSFC) (32400855 and 32300925), the STI 2030-Major Projects (2021ZD0201705), the Scientific Research Fund of Zhejiang Provincial Education Department (Y202249966), the Zhejiang Province Educational Science Planning Project (2024SCG018), the Starting Research Fund from Hangzhou Normal University (2021QDL079), the Eunice Kennedy Shriver National Institute of Child Health and Human Development (NICHD) (HD098235), the China Postdoctoral Science Foundation (2019M650884), and the Ministry of Science and Technology of the People's Republic of China (2021ZD0200505). The funders had no role in study design, data collection, and analysis, the decision to publish, or preparation of the manuscript. We thank Baoming Li, Jiefeng Jiang, Haiyan Wu, Fergus I.M. Craik, and Beatriz Luna for valuable suggestions on this manuscript. We also thank Jing Yang and Yifan Zhang for the data check of the extracted coordinates.

Author contributions

Zhenghan Li and Guochun Yang conceptualized the study. Guochun Yang, Joaquim Radua, and Zhenghan Li developed the methodology. Guochun Yang and Zhenghan Li conducted the formal analysis and curated the data. Zhenghan Li and Guochun Yang authored the original draft. Guochun Yang, Zhenghan Li, Isaac T. Petersen, Joaquim Radua, Lingxiao Wang, and Xun Liu contributed to the writing through review and editing. Funding was acquired by Zhenghan Li, Isaac T. Petersen, Xun Liu, and Guochun Yang. Guochun Yang supervised the research.

Data availability

The meta-data that support the findings of this study and all codes conducting the ROI analyses are available in Zenodo with the identifier doi: 10.5281/zenodo.15649138.

Appendix A. Supplementary material

Supplementary data to this article can be found online at https://doi.org/10.1016/j.scib.2025.08.038.

References

[1] Cohen JD. Cognitive control: core constructs and current considerations. In: Egner T, editor. The wiley handbook of cognitive control. Hoboken: Wiley Blackwell; 2017. p. 1–28.
[2] Li Z, Göschl F, Yang G. Dissociated neural mechanisms of target and distractor processing facilitated by expectations. J Neurosci 2020;40:1997–9.
[3] Constantinidis C, Luna B. Neural substrates of inhibitory control maturation in adolescence. Trends Neurosci 2019;42:604–16.
[4] Craik FIM, Bialystok E. Cognition through the lifespan: mechanisms of change. Trends Cognit Sci 2006;10:131–8.

[5] Zanto TP, Gazzaley A. Attention and ageing. In: Nobre K, editor. The oxford handbook of attention. New York: Oxford University Press; 2014. p. 927–71.
[6] American Psychiatric Association, DSM-5 Task Force. Diagnostic and statistical manual of mental disorders: Dsm-5™. 5th ed. Arlington: American Psychiatric Publishing, Inc.; 2013.
[7] Adnan A, Chen AJW, Novakovic-Agopian T, et al. Brain changes following executive control training in older adults. Neurorehabil Neural Repair 2017;31:910–22.
[8] Grady C. The cognitive neuroscience of ageing. Nat Rev Neurosci 2012;13:491–505.
[9] Weintraub S, Dikmen SS, Heaton RK, et al. Cognition assessment using the NIH toolbox. Neurology 2013;80:S54–64.
[10] Erb CD, Germine L, Hartshorne JK. Cognitive control across the lifespan: congruency effects reveal divergent developmental trajectories. J Exp Psychol Gen 2023;152:3285–91.
[11] Ferguson HJ, Brunsdon VEA, Bradford EEF. The developmental trajectories of executive function from adolescence to old age. Sci Rep 2021;11:1382.
[12] Bethlehem RAI, Seidlitz J, White SR, et al. Brain charts for the human lifespan. Nature 2022;604:525–33.
[13] Li Q, Yang G, Li Z, et al. Conflict detection and resolution rely on a combination of common and distinct cognitive control networks. Neurosci Biobehav Rev 2017;83:123–31.
[14] Giedd JN, Blumenthal J, Jeffries NO, et al. Brain development during childhood and adolescence: a longitudinal MRI study. Nat Neurosci 1999;2:861–3.
[15] Kerns JG, Cohen JD, MacDonald AW, et al. Anterior cingulate conflict monitoring and adjustments in control. Science 2004;303:1023–6.
[16] Neubauer AC, Fink A, Schrausser DG. Intelligence and neural efficiency. Intelligence 2002;30:515–36.
[17] Blakemore S-J. Imaging brain development: the adolescent brain. NeuroImage 2012;61:397–406.
[18] Crone EA, Dahl RE. Understanding adolescence as a period of social-affective engagement and goal flexibility. Nat Rev Neurosci 2012;13:636–50.
[19] Yaple ZA, Stevens WD, Arsalidou M. Meta-analyses of the n-back working memory task: fMRI evidence of age-related changes in prefrontal cortex involvement across the adult lifespan. NeuroImage 2019;196:16–31.
[20] Fernandez NB, Hars M, Trombetti A, et al. Age-related changes in attention control and their relationship with gait performance in older adults with high risk of falls. Neuroimage 2019;189:551–9.
[21] Verhaeghen P, Cerella J. Aging, executive control, and attention: a review of meta-analyses. Neurosci Biobehav Rev 2002;26:849–57.
[22] Reuter-Lorenz PA, Cappell KA. Neurocognitive aging and the compensation hypothesis. Curr Dir Psychol Sci 2008;17:177–82.
[23] Crone EA, Steinbeis N. Neural perspectives on cognitive control development during childhood and adolescence. Trends Cognit Sci 2017;21:205–15.
[24] Cabeza R. Hemispheric asymmetry reduction in older adults: the Harold model. Psychol Aging 2002;17:85–100.
[25] Park DC, Reuter-Lorenz P. The adaptive brain: aging and neurocognitive scaffolding. Annu Rev Psychol 2009;60:173–96.
[26] Wood G, Ischebeck A, Koppelstaetter F, et al. Developmental trajectories of magnitude processing and interference control: an fMRI study. Cereb Cortex 2009;19:2755–65.
[27] Hart H, Radua J, Nakao T, et al. Meta-analysis of functional magnetic resonance imaging studies of inhibition and attention in attention-deficit/hyperactivity disorder: exploring task-specific, stimulant medication, and age effects. JAMA Psychiat 2013;70:185–98.
[28] Zhang Z, Peng P, Eickhoff SB, et al. Neural substrates of the executive function construct, age-related changes, and task materials in adolescents and adults: ALE meta-analyses of 408 fMRI studies. Dev Sci 2021;24:e13111.
[29] Long J, Song X, Wang Y, et al. Distinct neural activation patterns of age in subcomponents of inhibitory control: a fMRI meta-analysis. Front Aging Neurosci 2022;14:938789.
[30] Miller EK, Cohen JD. An integrative theory of prefrontal cortex function. Annu Rev Neurosci 2001;24:167–202.
[31] Lu J, Yao J, Zhou Z, et al. Age effects on delay discounting across the lifespan: a meta-analytical approach to theory comparison and model development. Psychol Bull 2023;149:447–86.
[32] Page MJ, McKenzie JE, Bossuyt PM, et al. The PRISMA 2020 statement: an updated guideline for reporting systematic reviews. BMJ 2021;88:105906.
[33] Lancaster JL, Tordesillas-Gutierrez D, Martinez M, et al. Bias between MNI and Talairach coordinates analyzed using the ICBM-152 brain template. Hum Brain Mapp 2007;28:1194–205.
[34] Turkeltaub PE, Eickhoff SB, Laird AR, et al. Minimizing within-experiment and within-group effects in activation likelihood estimation meta-analyses. Hum Brain Mapp 2012;33:1–13.
[35] Müller VI, Cieslik EC, Laird AR, et al. Ten simple rules for neuroimaging meta-analysis. Neurosci Biobehav Rev 2018;84:151–61.
[36] Radua J, Mataix-Cols D. Meta-analytic methods for neuroimaging data explained. Biol Mood Anxiety Disord 2012;2:6.
[37] Albajes-Eizagirre A, Solanes A, Vieta E, et al. Voxel-based meta-analysis via permutation of subject images (PSI): theory and implementation for SDM. NeuroImage 2019;186:174–84.
[38] Hedges LV. Distribution theory for glass's estimator of effect size and related estimators. J Educ Behav Stat 1981;6:107–28.
[39] Zhang Z, Zhang Y, Wang H, et al. Resting-state network alterations in depression: a comprehensive meta-analysis of functional connectivity. Psychol Med 2025;55:e63.
[40] Zeng X, Han X, Gao F, et al. Abnormal structural alterations and disrupted functional connectivity in behavioral addiction: a meta-analysis of VBM and fMRI studies. J Behav Addict 2023;12:599–612.
[41] Eklund A, Nichols TE, Knutsson H. Cluster failure: why fMRI inferences for spatial extent have inflated false-positive rates. Proc Natl Acad Sci USA 2016;113:7900–5.
[42] Higgins JPT. Measuring inconsistency in meta-analyses. BMJ 2003;327:557–60.
[43] Wood SN. Mgcv: GAMs and generalized ridge regression for R. R News 2001;1:20–5.
[44] Zuo X-N, Kelly C, Di Martino A, et al. Growing together and growing apart: regional and sex differences in the lifespan developmental trajectories of functional homotopy. J Neurosci 2010;30:15034–43.
[45] Hoffman P, Morcom AM. Age-related changes in the neural networks supporting semantic cognition: a meta-analysis of 47 functional neuroimaging studies. Neurosci Biobehav Rev 2018;84:134–50.
[46] De Luca CR, Leventer RJ. Developmental trajectories of executive functions across the lifespan. In: Anderson V, Jacobs R, Anderson PJ, editors. Executive functions and the frontal lobes. New York: Psychology Press; 2010. p. 57–90.
[47] Bunge SA, Dudukovic NM, Thomason ME, et al. Immature frontal lobe contributions to cognitive control in children. Neuron 2002;33:301–11.
[48] Brenhouse HC, Andersen SL. Developmental trajectories during adolescence in males and females: a cross-species understanding of underlying brain changes. Neurosci Biobehav Rev 2011;35:1687–703.
[49] Casey B, Tottenham N, Liston C, et al. Imaging the developing brain: what have we learned about cognitive development? Trends Cognit Sci 2005;9:104–10.
[50] Luna B, Marek S, Larsen B, et al. An integrative model of the maturation of cognitive control. Annu Rev Neurosci 2015;38:151–70.
[51] Li S-C, Lindenberger U. Cross-level unification: a computational exploration of the link between deterioration of neurotransmitter systems and dedifferentiation of cognitive abilities in old age. In: Nilsson LG, Markowitsch HJ, editors. Cognitive neuroscience of memory. Seattle: Hogrefe & Huber Publishers; 1999. p. 103–46.
[52] Goh JOS. Functional dedifferentiation and altered connectivity in older adults: neural accounts of cognitive aging. Aging Dis 2011;2:30–48.
[53] Fjell AM, Walhovd KB. Structural brain changes in aging: courses, causes and cognitive consequences. Rev Neurosci 2010;21:187–221.
[54] Kaplan L, Chow BW, Gu C. Neuronal regulation of the blood–brain barrier and neurovascular coupling. Nat Rev Neurosci 2020;21:416–32.
[55] Zlokovic BV. Neurovascular pathways to neurodegeneration in Alzheimer's disease and other disorders. Nat Rev Neurosci 2011;12:723–38.
[56] Montalà-Flaquer M, Cañete-Massé C, Vaqué-Alcázar L, et al. Spontaneous brain activity in healthy aging: an overview through fluctuations and regional homogeneity. Front Aging Neurosci 2023;14:1002811.
[57] Zanto TP, Gazzaley A. Cognitive control and the ageing brain. In: Egner T, editor. The wiley handbook of cognitive control. Hoboken: Wiley Blackwell; 2017. p. 476–90.
[58] Prakash RS, Erickson KI, Colcombe SJ, et al. Age-related differences in the involvement of the prefrontal cortex in attentional control. Brain Cogn 2009;71:328–35.
[59] Chialvo DR, Zhang H-Y, Chen W-X, et al. Selective vulnerability related to aging in large-scale resting brain networks. PLoS One 2014;9:e108807.
[60] Thatcher RW, Walker RA, Giudice S. Human cerebral hemispheres develop at different rates and ages. Science 1987;236:1110–3.
[61] Grady CL, Bernstein LJ, Beig S, et al. The effects of encoding task on age-related differences in the functional neuroanatomy of face memory. Psychol Aging 2002;17:7–23.
[62] Zhou S-S, Fan J, Lee TMC, et al. Age-related differences in attentional networks of alerting and executive control in young, middle-aged, and older Chinese adults. Brain Cogn 2011;75:205–10.
[63] Mathis A, Schunck T, Erb G, et al. The effect of aging on the inhibitory function in middle-aged subjects: a functional MRI study coupled with a color-matched stroop task. Int J Geriatr Psychiatry 2009;24:1062–71.

Supplementary Text

Text S1. Detailed Description of the Features for Included Studies

The 125 articles included 139 studies (individual contrasts reported in the articles) with 3765 participants and 1685 activation foci reported. All studies were published or completed between January 1st 1994 and April 30th 2025. None of the experiments share the same group of participants. The included studies are written in English (135 studies) and Chinese (4 studies). Of the articles included, 123 were published in peer-reviewed journals, and 3 were master's theses. All included studies reported the task type used, including 77 studies utilizing Stroop-like task (55%), 26 studies utilizing Simon task (20%), 27 studies utilizing Flanker task (19%), 2 studies utilizing a combination of Simon and Flanker tasks (1%), 3 study utilizing a combination of Simon and Stroop tasks (2%), 3 studies utilizing multi-source interference task (2%), and 1 study utilizing a combination of Stroop and multi-source interference tasks (1%). In addition, the contrasts conducted to reveal brain activations were also reported, with 106 studies (77%) resulting from the contrast of Incongruent trials > Congruent trials, 27 studies (19%) resulting from the contrast of Incongruent trials > Neutral trials, and 6 studies (4%) resulting from the union contrast of Incongruent trials > Congruent trials and Incongruent trials > Neutral trials. Regarding the handedness of participants in the included studies, 97 studies (70%) included right-handed participants only, 6 studies (4%) included both left and right-handed participants, while 36 studies (26%) did not report this information. Furthermore, 84 studies (61%) included only correct response trials, 2 studies (1%) included both correct and incorrect response trials, while 53 studies (38%) did not report this information. Additionally, we obtained the behavioral congruency effect measured by reaction time from 131 studies (94%), with 2 studies (1%) did not measure the

reaction time and 6 studies (5%) measured but did not report the result. To eliminate the influence of these confounding factors, we included them as covariates in the modeling analyses.

Text S2. Regions Related to Cognitive Control Identified by ALE

To enhance the replicability and robustness of our findings, we also conducted the mean analysis across all studies with the activation likelihood estimation (ALE). We performed the single dataset analysis with the GingerALE software to explore the brain regions consistently reported in all the included studies (see section "*Spatial convergence using activation likelihood estimation (ALE)*" in Methods). Results showed significant activation in the frontoparietal regions, including the left dorsolateral prefrontal cortex, right frontal eye field, right inferior frontal gyrus (IFG) and right inferior parietal lobule (IPL); the cingulo-opercular regions, including the supplementary motor area and right insula; and other regions, including the left inferior temporal gyri (ITG), inferior occipital gyrus, and thalamus (Fig. S4 and Table S2).

Text S3. Validation of Using Mean Age as a Predictor in Meta-Regression

Previous meta-regression analyses have typically utilized averaged variables from each included study as predictors [1-3]. A potential concern with this approach is whether the average variable can effectively represent the entire sample, particularly when the range is extensive. In our study, the age ranges for most (~90%) studies are within 30 years, whereas some studies on young to middle-aged adults exhibited wider ranges (up to 59 years). To examine the efficacy of using mean age as a predictor in the meta-regression, we conducted a simulation analysis.

The logic behind this simulation parallels the seed-based *d* mapping with permutation of subject images (SDM-PSI) method [4], which estimates the overall effect size by simulating individual whole-brain activities based on the coordinate effect size data at the study level. By utilizing the average effect size and variance of both the age predictor and brain activity data, we generated simulated individual data to capture a spectrum of possibilities present in the original datasets. Through substantial repetitions, the average results from these individual simulations aimed to provide a reliable approximation of the actual results.

For each study, we generated a set of (n = sample size) individual data points from a normal distribution, defined by the study's mean and standard deviation (square root of variance). This process was conducted for both age and effect size. Simulated data for both variables were constrained within three standard deviations of the mean, with the age further constrained within reported ranges. When age ranges were not available, we used the following specific age brackets: 0 to 17 years for youth studies, 18 to 59 years for young to middle-aged adult studies, and 60 to 100 years for older adult studies. The latter constraint ensured that the simulated ages adhered to the respective age group definitions. The resulting simulated age data were used to predict the simulated effect size data through a mixed-effect generalized additive model (GAM), with both

the intercept and age predictor as random effects at the study level. To focus on the age effect, we did not include other covariates, such as the task types.

The estimates derived from the mixed-effect GAM were then employed to predict the effect size corresponding to each study's average age value. We correlated these predicted trajectories from the simulation with those from the group-level GAM meta-regression reported in the main text. The simulation process was repeated 1000 times to ensure robustness. The average correlation across all iterations was interpreted as a measure of overall efficacy.

We applied the simulation test on the nine regions of interest (ROIs) identified from the mean analysis, as these regions yielded more variance in their trajectory shapes. This diversity in the test data could improve the generalizability of our validation approach across different scenarios. Results suggested that, for 8 out of the 9 ROIs, the correlations between the trajectories predicted by the meta-regression and those from the simulated individual data were over 0.74 (3 regions reached over 0.91), indicating a substantially high level of agreement. The only deviation was observed in the left anterior cingulate cortex, where the correlation was 0.31. In this region, the meta-regression produced a linear trend (albeit not significant, as shown in Fig. 2), in contrast to the non-linear trend estimated in the simulated individual data. This discrepancy is likely due to the broader age ranges covered by the simulated data, which could lead to larger variance within a narrow age range. Visual comparisons of the trajectories further highlight strong consistencies between the simulation results and the meta-regression analyses (Fig. S5).

Overall, the simulation results indicate that meta-regression, which employs average age as a representative measure of the age range, accurately captures the age-related change patterns that are otherwise estimated with individual data.

Text S4. Testing the Significance of Peak Ages

With Simonsohn's [5] two-line approach, we tested whether the visually inverted U-shaped trajectories could be translated into two significant linear trends with opposite directions. We divided the data points into two sets (i.e., pre-peak and after-peak sets) with the peak age as the breaking point, and then conducted linear meta-regression analyses on each set. Given our specific hypothesis of an increasing slope before the peak and a decreasing slope afterward, we adopted one-tailed tests. The resulting *P* values were false discovery rate (FDR) corrected across the two sets and across the identified brain regions. We applied the same test to the peak ages from both the GAM and the simplified model fitting analyses.

Regarding regions identified in the mean analysis, we detected numerical peaks within the young to middle-aged range for two regions (r-ITG and r-MFG), which showed significant GAM results (Fig. 2). Both regions showed significant linear effects in the pre-peak phase, with *P*-FDRs < 0.022, but not in the post-peak phase, with *P*-FDRs > 0.060.

For the regions identified from the contrast analysis (Fig. 3), the peak ages calculated from the GAM analyses yielded significant linear relationships for both the pre-peak and post-peak sets, *P*-FDRs < 0.05, except the left IPL, which only showed a pre-peak linear increase, *P*-FDR < 0.001, but not post-peak, *P*-FDR $= 0.017$. Similarly, peak ages identified from the simplified modeling analyses yielded significant linear relationships for most of the regions, with *P*-FDRs < 0.05 for both pre- and post-peak sets; the only four exceptions were the right MTG, left IPL, which showed marginal significance in the post-peak sets, with *P*-FDRs values of 0.071 and 0.169, respectively. Note that while we did not explicitly label the peaks in the above regions showing marginal statistical significance, we considered them as potential peak candidates and included them in our main text analysis that correlated peaks between GAM and simplified modeling.

For the laterality analyses (Fig. S12), the "peak" age (defined as the smallest laterality across age, termed "peak" for consistency) calculated from both the GAM analysis and the square root model yielded significant linear relationships for the post-peak sets, Ps < 0.04, but not for the pre-peak set, Ps > 0.21.

Text S5. Contrast Results: Young to Middle-Aged Adults vs. the Youth and Young to Middle-Aged Adults vs. the Elderly

We conducted contrast analyses between the young-to-middle-aged adult group and the youth, as well as between the young-to-middle-aged adult group and the elderly, using the same SDM-PSI approach described in the main contrast analyses. For all comparisons, statistical significance was determined using a voxel-wise family-wise error (FWE) correction threshold of $P < 0.001$, with a minimum cluster extent of 100 voxels to ensure robust inference. We found that the young to middle-aged adult group showed significantly higher activation in certain regions compared to the youth group, including bilateral inferior frontal gyrus, bilateral inferior parietal lobule, left insula, right supplementary motor area, and right middle temporal gyrus. No significant regions showed a higher activation in the youth group than the young to middle-aged adult group (Fig. S7 and Table S8). Similarly, regions significantly more activated in the young to middle-aged adult group compared to the elderly group were revealed, including the left inferior parietal lobule, right inferior frontal gyrus, left insula, and left supplementary motor area. No significant regions showed higher activity in the elderly group than the young to middle-aged adult group (Fig. S10 and Table S8). In addition, there were no significant regions observed when comparing the youth group to the elderly group in either direction (Table S8).

In addition, we tested whether behavioral performance might influence the relative brain activity among the three groups. We conducted similar contrast analyses, but adding the covariate of the behavioral congruency effect measured by reaction time, along with an indicator regressor [6-8]. This analysis revealed consistent results as outlined above: young to middle-aged adults exhibited greater activation than the youth in the bilateral inferior frontal gyrus, bilateral inferior parietal lobule, left insula, left inferior temporal gyrus, right supplementary motor area, and right middle temporal gyrus, with no regions showing the opposite (Fig. S8 and Table S8).

Similarly, young to middle-aged adults showed stronger activation than the elderly in bilateral inferior parietal lobule, right inferior frontal gyrus, left insula, and left supplementary motor area, with no regions showing the opposite (Fig. S11 and Table S8). In addition, the youth showed no difference from the elderly. Overall, the consistency of these findings with the results before controlling for behavioral performance suggests that the observed weaker brain activations in the elderly and youth, compared to young to middle-aged adults, are robust.

In addition, we also conducted similar contrast analyses to the laterality measurement. This was achieved with linear meta-regression models: one comparing the youth with young to middle-aged adults, and the other comparing the elderly with young to middle-aged adults. In each model, we introduced a variable that encoded the specific groups of studies involved, designating the youth and elderly groups with a code of 1, and the young to middle-aged adult group with a code of −1. We also included covariates in other analyses to control for potential confounding factors, such as variations in task types. Results revealed that compared with the young to middle-aged adult group, both the elderly group (z = 1.92, P = 0.027, one-tailed, b = 0.23, 95% CI = [0.03, 0.42]), and the youth group showed greater left lateralization (z = 2.40, P = 0.008, one-tailed, b = 0.31, 95% CI = [0.10, 0.52]).

Text S6. Robustness Analyses

To ensure the robustness and validity of our findings, we performed several sensitivity analyses.

In our main text, we employed median imputation to handle missing data (9 studies, accounting for 6% of the total included studies) related to behavioral congruency effects. However, this approach may introduce bias if the imputed median values differ significantly from the true data. To assess its potential impact on our conclusions, we compared results obtained after removing these studies and those obtained using median imputation for the behavioral congruency effects. We focused on testing the key findings of the inverted U-shaped trajectories observed between young to middle-aged adults and the other groups. To test this, we reanalyzed the fitting process for brain regions identified in the contrast analysis of young to middle-aged adults vs. other groups (Fig. 3) by removing the 9 studies with missing data. The results showed that the GAM significantly fitted all regions with smooth curves, Fs > 8.5, Ps < 0.001, FDR corrected, with degrees of freedom varying from 3.6 to 5.0. Using simplified models, we found that the square root model continued to best describe the data. These results exactly replicated the results using imputation, suggesting that our findings based on the imputation method are robust.

It has been suggested that the inclusion of unpublished and non-English studies in meta-analyses can reduce potential bias [9,10]. However, this practice may also introduce variations in the results. Our study incorporated three unpublished master's theses and four non-English studies written in Chinese. To test their influence, we performed a meta-regression analysis after excluding these studies, using regions identified by the mean analysis of SDM. Given that all three unpublished studies were also non-English (a total of four), we excluded both from the reanalysis due to significant overlap. Results showed that GAM significantly fitted the age-related changes in activation levels for 2 out of the 6 regions, Ps < .05, FDR corrected (Fig. S6, r-ITG and r-MFG),

and the other six regions showed no significant age-related changes. These results exactly replicate the original findings. Thus, the inclusion of unpublished and non-English studies has a limited impact on our meta-analysis results.

Furthermore, to assess the potential impact of missing studies within the 45–60 age range on the mean results, we conducted a mean analysis including the age as a covariate using the SDM-PSI. This analysis reaffirmed the same brain clusters previously identified (see Fig. S3 and Table S3). This suggests that the missing studies have limited influence on the mean results.

Text S7. Lifespan Trajectory of the Behavioral Performance

We also tested how the behavioral congruency effect (measured by RT) changes with age, using analytical methods similar to the laterality analysis but with the following adjustments: (1) the dependent variable was the RT-based congruency effect, (2) congruency-related covariates were removed, and (3) studies not reporting behavioral results were excluded.

First, we modeled the age-related trajectory using the GAM. The result was not significant, $F(1.0, 1.0) = 0.42$, $P = 0.520$, $R^2 = 0.00$. We then tested the four simplified models (i.e., the quadratic, cubic, square root, and quadratic logarithmic models), none of which fit the data significantly (ps > 0.61). A further comparison across age groups revealed that the youth group (103.4 ms) exhibited only numerically larger congruency effects than the young to middle-aged adult group (90.9 ms), $P = 0.18$, and the elderly group (108.8 ms) also showed a nonsignificant numerical increase, $P = 0.34$. The scatter plot of behavioral performance is shown in Fig. S13.

The lack of significant age-related differences in the behavioral congruency effect might be attributed to several factors. First, behavioral measurements might be sensitive to the exact experimental designs. Second, we were limited to analyzing raw congruency effects because most studies did not report the standard deviations specifically for the congruency effect (the critical contrast needed for effect size calculation). Third, by including only studies with concurrent fMRI data, we excluded a substantial number of behavioral-only studies, which may have reduced the representativeness of our sample. Therefore, caution is needed when interpreting behavioral results from this fMRI-focused subset. Future research would benefit from using standardized effect sizes and including a broader range of study designs.

Supplementary Discussion

Implications of Our Finding for Other Cognitive Control Subdomains

A more comprehensive understanding of the lifespan trajectory of cognitive control relies on studying different subdomains of cognitive control, such as conflict processing, working memory, and cognitive flexibility [11]. Previous studies have suggested that different subdomains of cognitive control exhibit both similar and separable neural mechanisms [12]. Moreover, these subdomains might follow different lifespan trajectories [13]. Findings from our study may contribute valuable insights into the potential differences in brain activity across different components of cognitive control during development.

Consistent with the inverted U-shaped trajectory, we confirmed that the young adults exhibit higher levels of cognitive control brain activities compared to the youth during conflict processing but not otherwise (supplementary Fig. S7, Table S8). This observation is in line with previous studies [14–18]. To the best of our knowledge, previous research using conflict tasks has rarely reported findings that contradict this direction (except [19]). However, more controversial patterns have emerged in studies focusing on other subdomains of cognitive control, such as working memory [20–22] and response inhibition [23–25]. For instance, with visual-spatial working memory task, Scherf, et al. [20] found an age-related increase in the recruitment of brain regions in the lateral prefrontal cortex, whereas Geier, et al. [22] reported both age-related increase and decrease in different prefrontal regions. These studies employed similar paradigms but different contrast methods (i.e., delay vs. non-delay and long-delay vs. short-delay), which exemplifies the many diversities within the working memory domain [26]. Similarly, in the subdomain of response inhibition, studies have shown discrepancies in brain engagement with different designs and different measurements [27,28]. On the contrary, conflict processing provides a more consistent

framework for measuring brain activities across age groups. Given these differences, it is prudent to be cautious in generalizing our current findings to the lifespan trajectories of other subdomains of cognitive control, although an inverted U-shaped trajectory could be a good candidate hypothesis to begin with. Future research is necessary to develop more precise cross-age comparisons within these other cognitive control subdomains.

Supplementary Figures

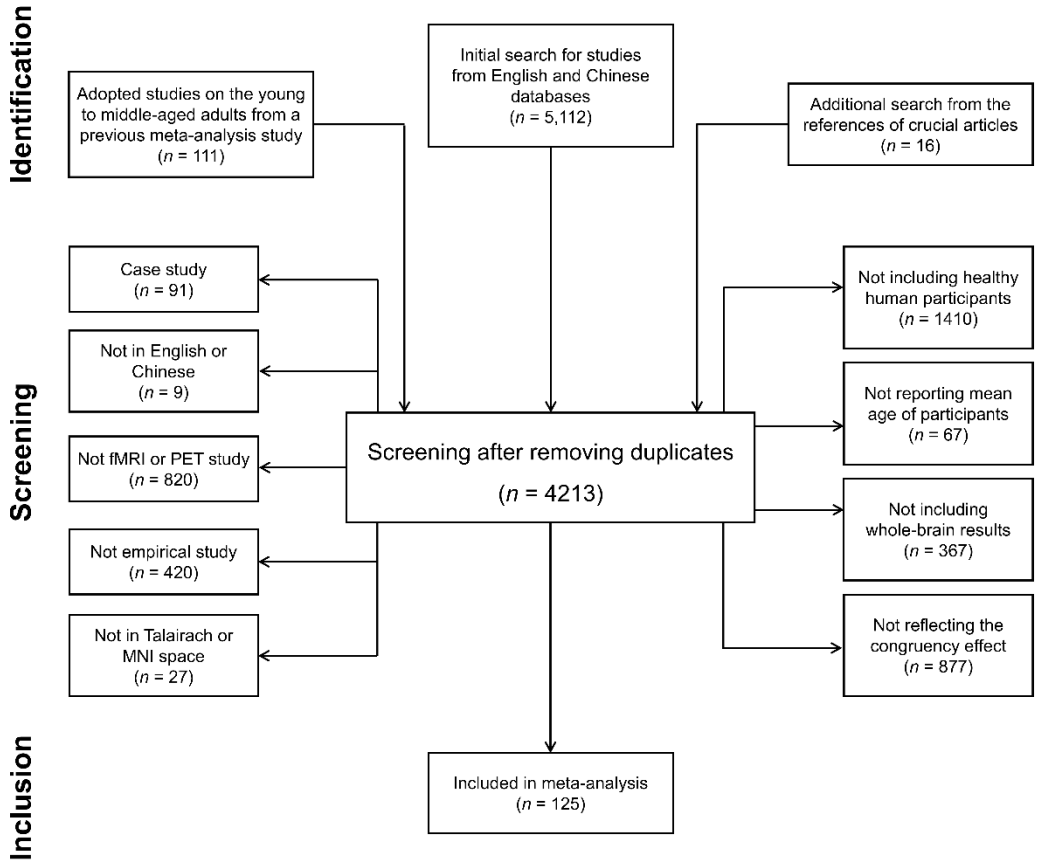

Fig. S1. The preferred reporting items for systematic reviews and meta-analyses flowchart of the selection process for included articles. fMRI = functional magnetic resonance imaging; PET = positron emission tomography; MNI = Montreal Neurological Institute.

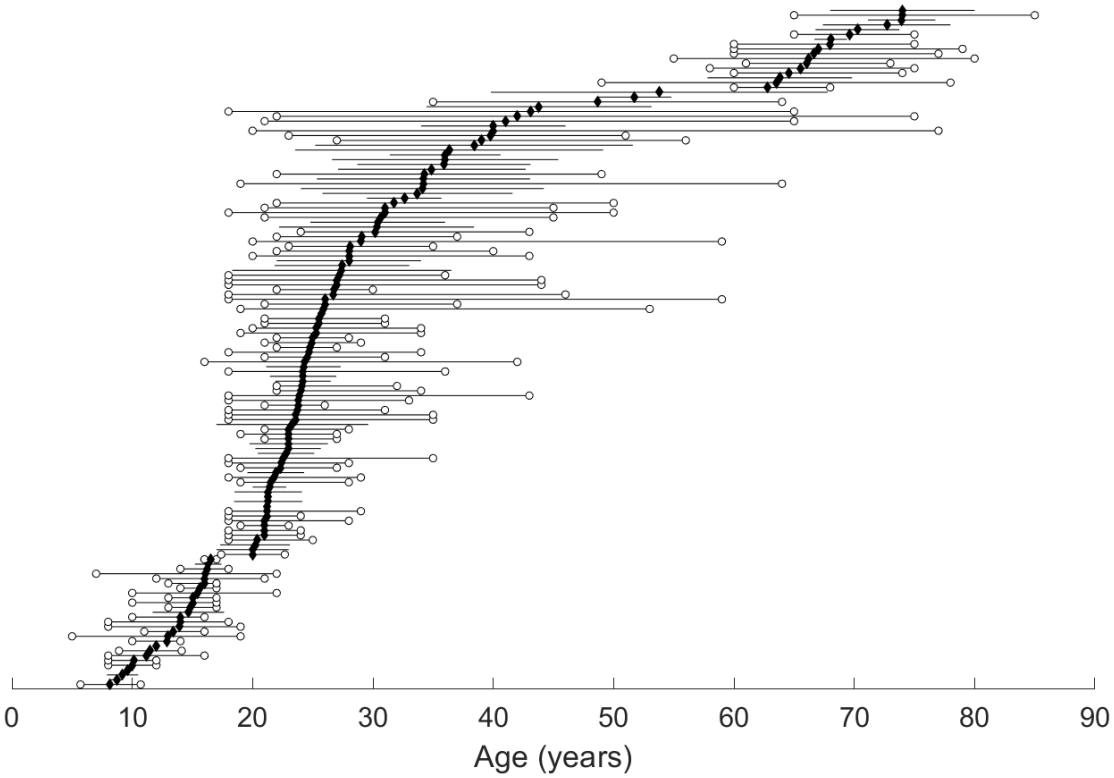

Fig. S2. Age distribution of included studies. Black diamonds denote mean ages, lines with open circles denote age ranges, and lines without open circles denote standard deviations. Ages are sorted with the mean age of each study.

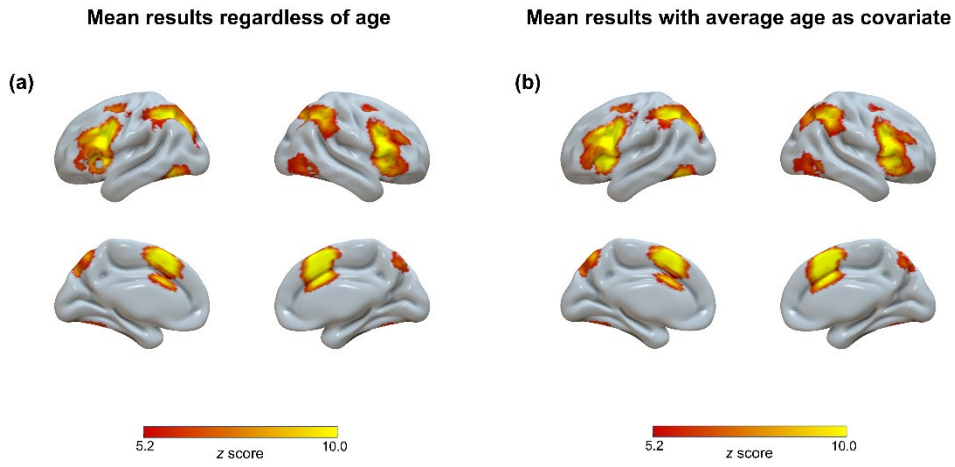

Fig. S3. Significant clusters (voxel-wise FWE-corrected, $P < 0.001$, with minimum cluster size ≥ 100 voxels) across all studies in the SDM meta-analysis regardless of age (a) and with average age as covariate (b).

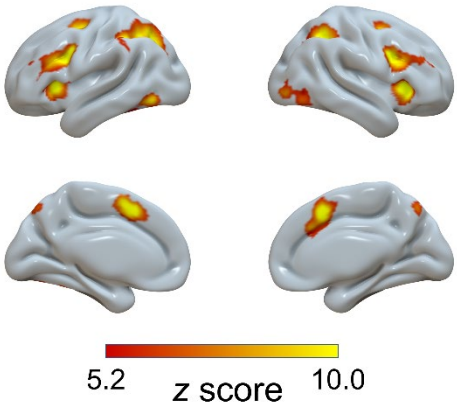

Fig. S4. Regions related to cognitive control identified by ALE (voxel-wise FWE-corrected, $P < 0.001$, with minimum cluster size ≥ 100 voxels) across all studies.

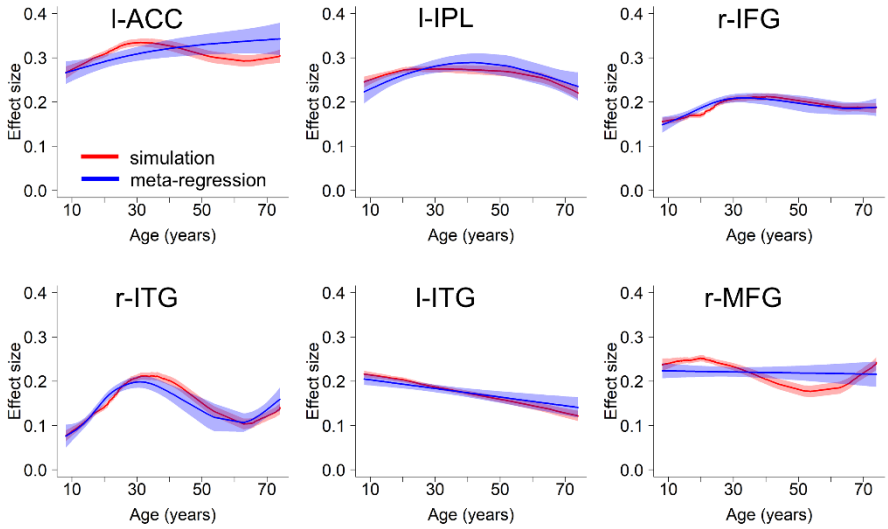

Fig. S5. Trajectories predicted by the simulation (red) and meta-regression (blue). The trajectory of meta-regression was consistent with what was reported in Fig. 2 of the main text, except that in panels l-ACC, l-IPL, r-IFG, and l-ITG, where the fitted curves were not plotted in Fig. 2 due to insignificant GAM fitting results. The simulation predicted curves derive from the simulated individual data, with the illustrated trajectories representing the average curves across 1000 iterations. Shaded regions around these curves represent standard errors. l-ACC: left anterior cingulate cortex, l-IPL: left inferior parietal lobule, r-IFG: right inferior frontal gyrus, r-ITG: right inferior temporal gyrus, l-ITG: left inferior temporal gyrus, r-MFG: right middle frontal gyrus.

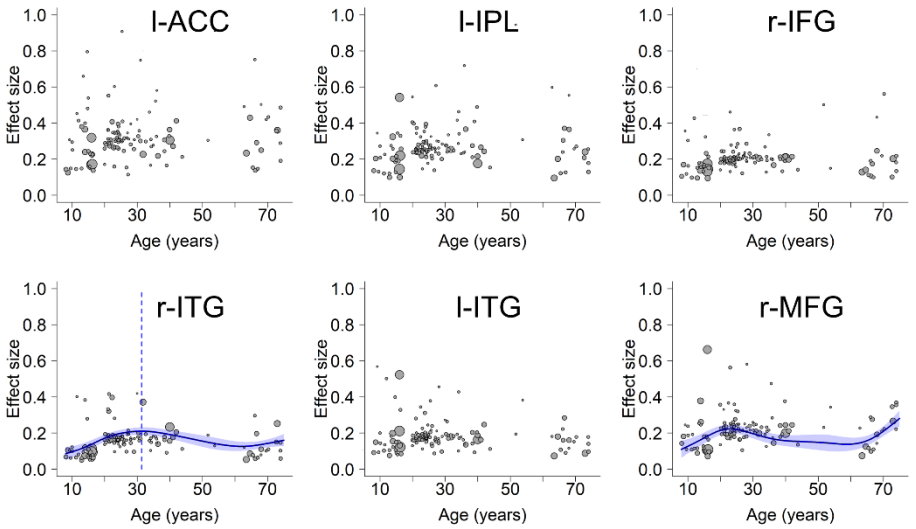

Fig. S6. Robustness analysis of lifespan trajectories within regions identified in the mean analysis, with the unpublished and non-English studies excluded. l-ACC: left anterior cingulate cortex, l-IPL: left inferior parietal lobule, r-IFG: right inferior frontal gyrus, r-ITG: right inferior temporal gyrus, l-ITG: left inferior temporal gyrus, r-MFG: right middle frontal gyrus. Scattered plots are the effect sizes as a function of age, with curves fitted by GAM. The sizes of the scattered dots show the square root of model weights (1/variance) for each study. Shaded areas around the curves represent standard errors. Dashed lines indicate peak ages. Regions not showing the peak age are due to insignificant two-line tests.

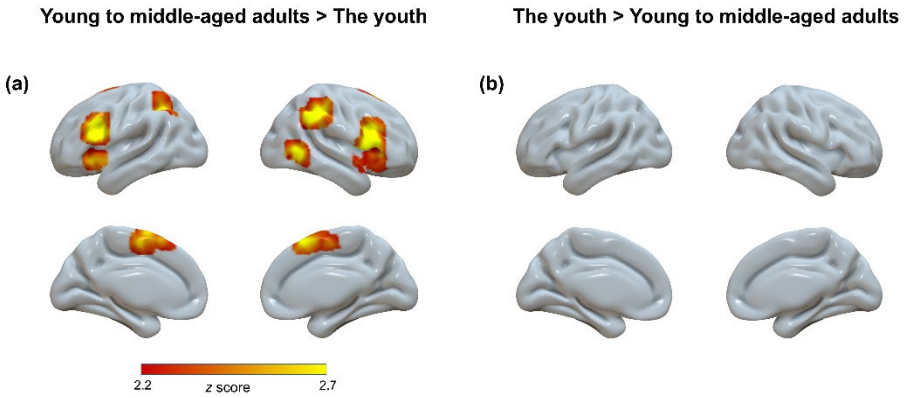

Fig. S7. Significant clusters (voxel-wise FWE-corrected, $P < 0.001$, with minimum cluster size ≥ 100 voxels) for contrast analyses between the young to middle-aged adult group and the youth group. The displayed regions show higher activities in young to middle-aged adults than the youth (a). No regions show the opposite direction (b).

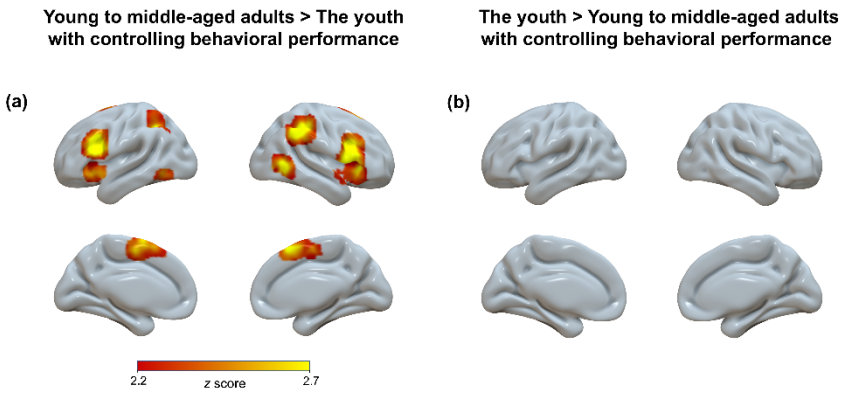

Fig. S8. Significant clusters (voxel-wise FWE-corrected, $P < 0.001$, with minimum cluster size ≥ 100 voxels) for contrast analyses between the young to middle-aged adult group and the youth group with controlling behavioral performance. The displayed regions show higher activities in young to middle-aged adults than the youth (a). No regions show the opposite direction (b).

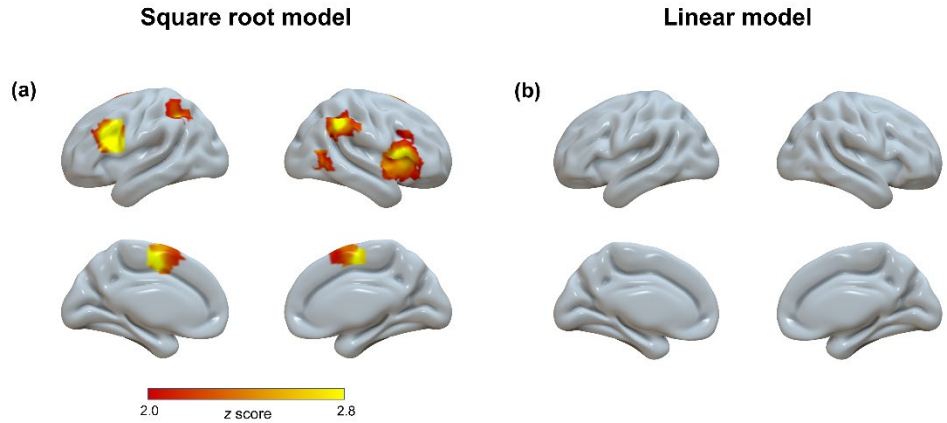

Fig. S9. Significant clusters (voxel-wise FWE-corrected, $P < 0.001$, voxels ≥ 100) showing square root pattern (a) and linear pattern (b) with age in the model fitting.

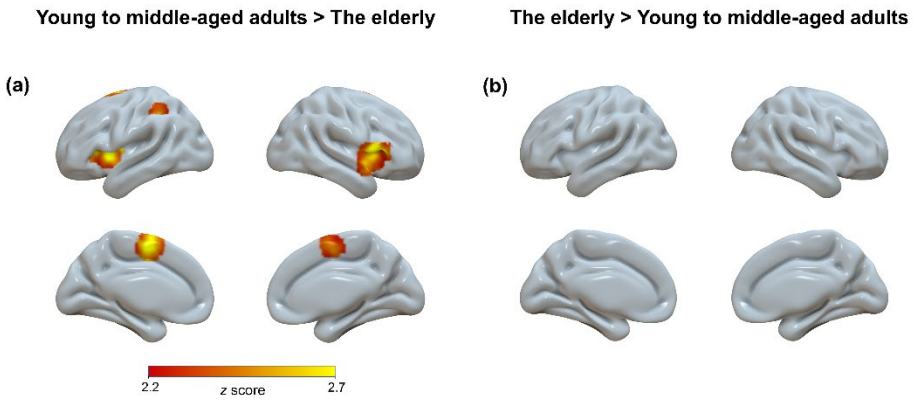

Fig. S10. Significant clusters (voxel-wise FWE-corrected, $P < 0.001$, with minimum cluster size ≥ 100 voxels) for contrast analyses between the young to middle-aged adult group and the elderly group. The displayed regions show higher activities in younger adults than older adults (a). No regions show the opposite direction (b).

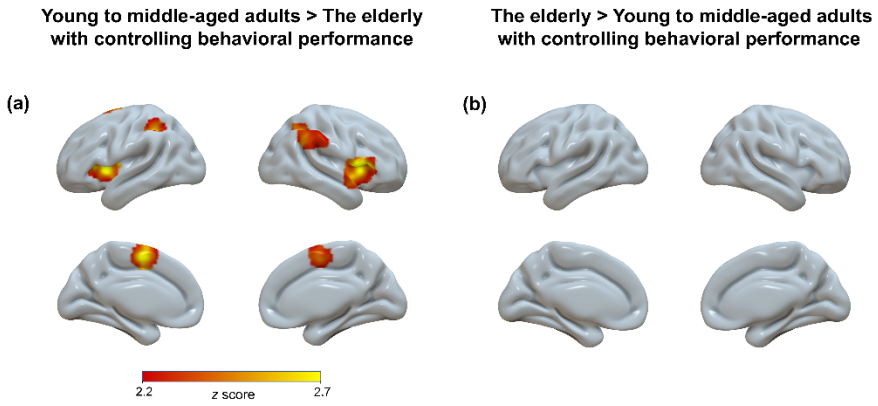

Fig. S11. Significant clusters (voxel-wise FWE-corrected, $P < 0.001$, with minimum cluster size ≥ 100 voxels) for contrast analyses between the young to middle-aged adult group and the elderly group with controlling behavioral performance. The displayed regions show higher activities in younger adults than older adults (a). No regions show the opposite direction (b).

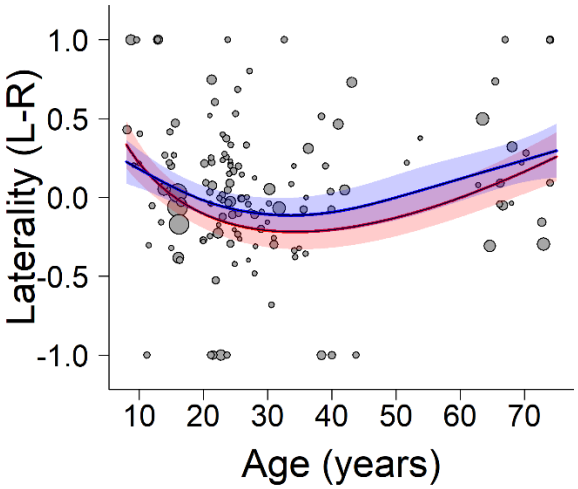

Fig. S12. Scatter plot of the lifespan trajectory of the laterality. A visually upright U-shaped trajectory indicated the youth and elderly adults tended to be more left-lateralized across the whole brain.

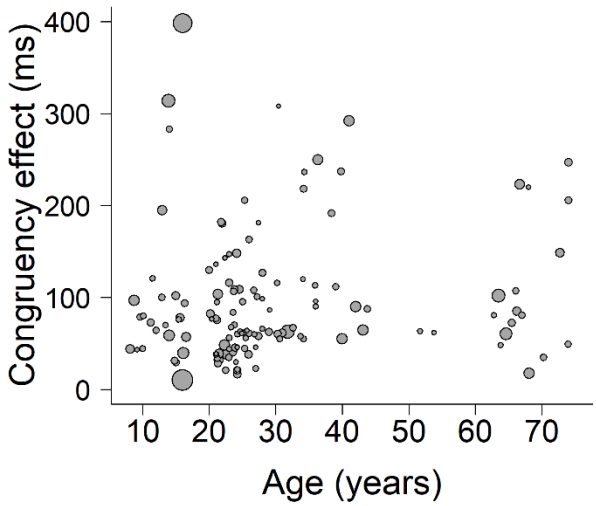

Fig. S13. Scatter plot of the behavioral performance defined by reaction time-indexed congruency effect. Note that studies not reported behavioral results are removed from the analysis.

Supplementary Tables

Table S1. Studies included in the present study. (Available as a separate supplementary Excel file.)

Table S2. Activation across all age groups with ALE (voxel-level cluster-forming $P < 0.001$ and cluster-level FWE-corrected $P < 0.05$).

Order	# Voxels	ALE ($\times 10^{-2}$)	*P*	L/R	MNI coordinate			Anatomical location	BA
					x	y	z		
1	3467	8.50	< 0.001	R	34	−52	46	Inferior parietal lobule	7
2	2523	10.67	< 0.001	L	−42	4	32	Dorsolateral prefrontal cortex	6
3	2425	7.48	< 0.001	/	0	14	48	Pre-supplementary motor area	32
4	1260	10.55	< 0.001	R	46	10	30	Inferior frontal gyrus	9
5	1158	9.92	< 0.001	R	36	24	−2	Insula	13
6	576	6.73	< 0.001	L	−44	−66	−10	Inferior temporal gyrus	37
7	490	4.70	< 0.001	R	40	−86	−4	Inferior occipital gyrus	18
8	359	6.42	< 0.001	R	26	0	52	Frontal eye field	6
9	292	4.51	< 0.001	L	−12	−16	8	Thalamus	/

Note. ALE = activation likelihood estimation; MNI = Montreal Neurological Institute; BA = Brodmann area; L = left; R = right.

Table S3. Activation across all age groups with SDM (voxel-wise FWE-corrected, $P < 0.001$, with minimum cluster size ≥ 100 voxels).

Order	# Voxels	*Z*	*P*	L/R	MNI coordinate			Anatomical location	BA
					x	y	z		
Mean results regardless of age									
1	10061	12.776	< 0.001	L	−2	28	38	Anterior cingulate cortex	32
2	7638	12.419	< 0.001	L	−34	−62	44	Inferior parietal lobule	7
3	5095	12.637	< 0.001	R	50	20	4	Inferior frontal gyrus	45
4	1855	8.560	< 0.001	R	52	−60	−12	Inferior temporal gyrus	37
5	1585	9.769	< 0.001	L	−46	−62	−12	Inferior temporal gyrus	37
6	382	7.684	< 0.001	R	30	0	58	Middle frontal gyrus	6
Mean results with average age as covariate									
1	10863	12.757	< 0.001	L	−2	20	34	Anterior cingulate cortex	24
2	8298	12.633	< 0.001	L	−36	−62	44	Inferior parietal lobule	7
3	5180	13.212	< 0.001	R	50	18	4	Inferior frontal gyrus	45
4	2011	8.883	< 0.001	R	54	−60	−10	Inferior temporal gyrus	37
5	1703	9.709	< 0.001	L	−46	−62	−12	Inferior temporal gyrus	37
6	331	6.805	< 0.001	R	32	6	52	Middle frontal gyrus	6

Note. MNI = Montreal Neurological Institute; BA = Brodmann area; L = left; R = right.

Table S4. The fitting results of the GAM analyses.

Order	Region name	Estimated degree of freedom	Peak age	*F*	Effect size
Peak-based regions identified in the mean analysis with SDM					
1	Anterior cingulate cortex	1.0	/	0.36	0.00
2	Inferior parietal lobule	3.2	/	1.96	0.05
3	Inferior frontal gyrus	2.3	/	1.38	0.02
4	Inferior temporal gyrus	3.9	31.2	5.72	0.17
5	Inferior temporal gyrus	1.0	/	4.09	0.02
6	Middle frontal gyrus	4.5	/	3.54	0.07
Regions identified in the contrast analysis of Young to middle-aged adults > Others					
1	Inferior frontal gyrus	4.2	30.7	17.93	0.40
2	Inferior parietal lobule	4.0	32.8	15.66	0.35
3	Supplementary motor area	4.0	27.7	10.06	0.25
4	Inferior frontal gyrus	5.0	28.7	10.78	0.29
5	Inferior parietal lobule	3.7	/	11.36	0.24
6	Middle temporal gyrus	4.7	35.7	23.66	0.44
7	Insula	4.0	30.6	8.55	0.22

Note. Peak-based regions are defined by sphere masks centered in the peak coordinates identified from the Mean analysis, whereas the regions identified in the contrast analysis of Young to middle-aged adults > Others are the original areas from the contrast analysis between young to middle-aged adults and other age groups (Table 1). Effect sizes are measured by the difference in adjusted R^2 between full and reduced models (with vs. without the s(age) term).

Table S5. Weights of each model based on AIC values.

Order	Region name	Qua	Cub	QuaLog	Sqrt
1	Inferior frontal gyrus	0.286	0.069	0.221	0.424*
2	Inferior parietal lobule	0.251	0.064	0.277	0.407*
3	Supplementary motor area	0.212	0.062	0.351	0.375*
4	Inferior frontal gyrus	0.26	0.05	0.277	0.412*
5	Inferior parietal lobule	0.269	0.059	0.27	0.402*
6	Middle temporal gyrus	0.345	0.054	0.216	0.384*
7	Insula	0.221	0.088	0.299	0.392*

Note. Regions are from the contrast analysis between young to middle-aged adults and other age groups (Table 1). Qua = quadratic model; Cub = cubic model; QuaLog = quadratic logarithmic model; Sqrt = square root model. * denotes the model with the highest weight.

Table S6. The results of the optimal model fitting.

Order	Region name	Best model	QM	*P*	Peak age	Fixed effect	95% Confidence interval
1	Inferior frontal gyrus	Square root	21.41	< 0.001	32.6	0.33	[0.14,0.52]
2	Inferior parietal lobule	Square root	19.59	< 0.001	33.9	0.31	[0.12,0.50]
3	Supplementary motor area	Square root	19.63	0.003	33.1	0.27	[0.08,0.46]
4	Inferior frontal gyrus	Square root	28.99	< 0.001	35.0	0.33	[0.14,0.52]
5	Inferior parietal lobule	Square root	23.63	< 0.001	/	0.31	[0.12,0.50]
6	Middle temporal gyrus	Square root	15.06	0.003	33.8	0.27	[0.08,0.45]
7	Insula	Square root	22.49	0.002	33.8	0.29	[0.10,0.48]

Note. Regions are from the contrast analysis between young to middle-aged adults and other age groups (Table 1). QM is the test statistic of the Wald-type test of the model coefficients; *P* is the statistical significance of the sqrt(age) term from the Square root model.

Table S7. Brain areas exhibiting a square root lifespan trajectory (voxel-wise FWE-corrected, $P < 0.001$, with minimum cluster size ≥ 100 voxels).

Order	# Voxels	*Z*	*P*	L/R	MNI coordinate			Anatomical location	BA
					x	y	z		
1	1781	4.797	< 0.001	R	50	18	4	Inferior frontal gyrus	45
2	800	5.006	< 0.001	L	−44	16	24	Inferior frontal gyrus	48
3	784	4.075	< 0.001	R	52	−46	38	Inferior parietal lobule	/
4	426	3.408	< 0.001	/	0	−4	56	Supplementary motor area	48
5	421	3.804	< 0.001	L	−34	−50	42	Inferior parietal lobule	40
6	147	3.458	< 0.001	R	56	−58	0	Middle temporal gyrus	/

Note. MNI = Montreal Neurological Institute; BA = Brodmann area; L = left; R = right.

Table S8. Overview of significant clusters in two-group contrast analyses between the youth, young to middle-aged adult, and the elderly groups (voxel-wise FWE-corrected, $P < 0.001$, with minimum cluster size ≥ 100 voxels) with SDM.

Order	# Voxels	*Z*	*P*	L/R	MNI coordinate			Anatomical location	BA
					x	y	z		
Young to middle-aged adults > The youth									
1	1617	4.037	< 0.001	R	54	16	10	Inferior frontal gyrus	48
2	1166	4.510	< 0.001	R	38	−42	40	Inferior parietal lobule	40
3	823	3.316	< 0.001	R	10	20	56	Supplementary motor area	/
4	695	4.562	< 0.001	L	−44	14	26	Inferior frontal gyrus	48
5	400	3.580	< 0.001	L	−36	−52	42	Inferior parietal lobule	40
6	195	3.758	< 0.001	R	52	−62	2	Middle temporal gyrus	37
7	146	2.969	< 0.001	L	−38	24	−6	Insula	47
The youth > Young to middle-aged adults									
None									
Young to middle-aged adults > The youth with controlling behavioral performance									
1	1727	4.037	< 0.001	R	54	16	10	Inferior frontal gyrus	48
2	1180	4.268	< 0.001	R	38	−42	40	Inferior parietal lobule	40
3	690	4.598	< 0.001	L	−44	16	24	Inferior frontal gyrus	48
4	809	3.337	< 0.001	R	10	20	56	Supplementary motor area	/
5	354	3.374	< 0.001	L	−34	−52	36	Inferior parietal lobule	/
6	186	3.648	< 0.001	R	52	−62	2	Middle temporal gyrus	37
7	143	2.971	< 0.001	L	−38	24	−6	Insula	47
8	103	3.109	< 0.001	L	−52	−64	−12	Inferior temporal gyrus	37
The youth > Young to middle-aged adults with controlling behavioral performance									
None									

Young to middle-aged adults > The elderly

1	1191	4.388	< 0.001	R	46	10	0	Inferior frontal gyrus	48
2	492	3.245	< 0.001	L	−32	8	2	Insula	48
3	432	3.265	< 0.001	L	−10	0	62	Supplementary motor area	/
4	136	3.305	< 0.001	L	−40	−40	40	Inferior parietal lobule	40

The elderly > Young to middle-aged adults

None

Young to middle-aged adults > The elderly with controlling behavioral performance

1	1309	4.296	< 0.001	R	48	12	0	Inferior frontal gyrus	48
2	521	3.218	< 0.001	L	−32	8	2	Insula	48
3	424	3.191	< 0.001	L	−10	2	60	Supplementary motor area	/
4	218	3.285	< 0.001	L	−38	−40	42	Inferior parietal lobule	40
5	158	2.774	< 0.001	R	54	−48	40	Inferior parietal lobule	6
6	129	3.090	< 0.001	R	30	−52	40	Inferior parietal lobule	/

The elderly > Young to middle-aged adults with controlling behavioral performance

None

The youth > The elderly

None

The elderly > The youth

None

The youth > The elderly with controlling behavioral performance

None

The elderly > The youth with controlling behavioral performance

None

Note. MNI = Montreal Neurological Institute; BA = Brodmann area; L = left; R = right.

References

[1] Yaple ZA, Stevens WD, Arsalidou M. Meta-analyses of the n-back working memory task: fMRI evidence of age-related changes in prefrontal cortex involvement across the adult lifespan. NeuroImage 2019; 196: 16-31.

[2] Lu J, Yao J, Zhou Z, et al. Age effects on delay discounting across the lifespan: A meta-analytical approach to theory comparison and model development. Psychol Bull 2023; 149: 447-486.

[3] Ho RC, Cheung MW, Fu E, et al. Is high homocysteine level a risk factor for cognitive decline in elderly? A systematic review, meta-analysis, and meta-regression. Am J Geriatr Psychiatry 2011; 19: 607-617.

[4] Albajes-Eizagirre A, Solanes A, Vieta E, et al. Voxel-based meta-analysis via permutation of subject images (PSI): Theory and implementation for SDM. NeuroImage 2019; 186: 174-184.

[5] Simonsohn U. Two lines: A valid alternative to the invalid testing of u-shaped relationships with quadratic regressions. Adv Meth Pract Psych 2018; 1: 538-555.

[6] Ochieng' Odhiambo F. Comparative study of various methods of handling missing data. Mathematical Modelling and Applications 2020; 5: 87-93.

[7] Tsikriktsis N. A review of techniques for treating missing data in om survey researchJ Oper Manag 2005; 24: 53-62.

[8] Sandhu AT, Kohsaka S, Turakhia MP, et al. Evaluation of quality of care for us veterans with recent-onset heart failure with reduced ejection fraction. JAMA Cardiol 2022; 7: 130-139.

[9] Cumpston M, Li T, Page MJ, et al. Updated guidance for trusted systematic reviews: A new edition of the cochrane handbook for systematic reviews of interventions. Cochrane Database Syst Rev 2019; 10: ED000142.

[10] Polanin JR, Tanner-Smith EE, Hennessy EA. Estimating the difference between published and unpublished effect sizes. Rev Educ Res 2016; 86: 207-236.

[11] Diamond A. Executive functions. Annu Rev Psychol 2013; 64: 135-168.

[12] He L, Zhuang K, Chen Q, et al. Unity and diversity of neural representation in executive functions. J Exp Psychol Gen 2021; 150: 2193-2207.

[13] Ferguson HJ, Brunsdon VEA, Bradford EEF. The developmental trajectories of executive function from adolescence to old age. Sci Rep 2021; 11: 1382.

[14] Andrews-Hanna JR, Mackiewicz Seghete KL, Claus ED, et al. Cognitive control in adolescence: Neural underpinnings and relation to self-report behaviors. PLoS One 2011; 6: e21598.

[15] Veroude K, Jolles J, Croiset G, et al. Changes in neural mechanisms of cognitive control during the transition from late adolescence to young adulthood. Dev Cogn Neurosci 2013; 5: 63-70.

[16] Wilk HA, Morton JB. Developmental changes in patterns of brain activity associated with moment-to-moment adjustments in control. Neuroimage 2012; 63: 475-484.

[17] Konrad K, Neufang S, Thiel CM, et al. Development of attentional networks: An fMRI study with children and adults. Neuroimage 2005; 28: 429-439.

[18] Marsh R, Zhu H, Schultz RT, et al. A developmental fmri study of self-regulatory control. Hum Brain Mapp 2006; 27: 848-863.

[19] Bunge SA, Dudukovic NM, Thomason ME, et al. Immature frontal lobe contributions to cognitive control in children. Neuron 2002; 33: 301-311.
[20] Scherf KS, Sweeney JA, Luna B. Brain basis of developmental change in visuospatial working memory. J Cogn Neurosci 2006; 18: 1045-1058.
[21] Olesen PJ, Macoveanu J, Tegner J, et al. Brain activity related to working memory and distraction in children and adults. Cereb Cortex 2007; 17: 1047-1054.
[22] Geier CF, Garver K, Terwilliger R, et al. Development of working memory maintenance. J Neurophysiol 2009; 101: 84-99.
[23] Booth JR, Burman DD, Meyer JR, et al. Neural development of selective attention and response inhibition. Neuroimage 2003; 20: 737-751.
[24] Durston S, Davidson MC, Tottenham N, et al. A shift from diffuse to focal cortical activity with development. Dev Sci 2006; 9: 1-8.
[25] Rubia K, Smith AB, Woolley J, et al. Progressive increase of frontostriatal brain activation from childhood to adulthood during event-related tasks of cognitive control. Hum Brain Mapp 2006; 27: 973-993.
[26] Rottschy C, Langner R, Dogan I, et al. Modelling neural correlates of working memory: A coordinate-based meta-analysis. Neuroimage 2012; 60: 830-846.
[27] Criaud M, Boulinguez P. Have we been asking the right questions when assessing response inhibition in go/no-go tasks with fmri? A meta-analysis and critical review. Neurosci Biobehav Rev 2013; 37: 11-23.
[28] Simmonds DJ, Pekar JJ, Mostofsky SH. Meta-analysis of go/no-go tasks demonstrating that fmri activation associated with response inhibition is task-dependent. Neuropsychologia 2008; 46: 224-232.

Order	First author	Year	Publication type	Task type	Experimental design	Sample size (female)	Language	Mean age (SD) (years)	Age range (years)	Handness	Contrast	Correct trials only	Congruency effect (RT, ms)
The youth													
1	Andrews-Hanna	2011	Journal	Stroop task	Hybrid block/event-related design	32 (15)	English	15.6 (*n.r.*)	14−17	right	I > N	Yes	78
2	Bernal	2009	Journal	Stroop task	Hybrid block/event-related design	18 (10)	English	14.67 (2.97)	*n.r.*	right	I > C	*n.r.*	*n.r.*
3	Bunge	2002	Journal	Flanker task	Event-related design	16 (6)	English	10 (*n.r.*)	8−12	right	I > N	Yes	44.4
4	Cao	2006	Journal	rhyming task (Stroop-like)	Event-related design	14 (6)	English	11.5 (*n.r.*)	8.9−14.11	right	I > N	No	121
5	Carp	2012	Journal	multi-source interference task	Event-related design	18 (8)	English	14 (*n.r.*)	8−18	*n.r.*	I > C	Yes	283.3
6	deKieviet	2014	Journal	Flanker task	Block design	47 (26)	English	8.7 (0.5)	*n.r.*	*n.r.*	I > C	n.r.	97
7	Fan	2014	Journal	Stroop task	Event-related design	23 (2)	English	11.2 (2.9)	8−16	*n.r.*	I > C	*n.r.*	73
8	Gee	2022	Journal	Stroop task	Block design	40 (22)	English	12.93 (3.92)	5−19	right	I > C	*n.r.*	195.04
9	Halari	2009	Journal	Simon task	Event-related design	21 (11)	English	16.3 (1.1)	14−17	*n.r.*	I > C	*n.r.*	94
10	Hansen	2018	Journal	Stroop task	Block design	171 (50)	English	16.2 (1)	14−18	*n.r.*	I > C	*n.r.*	*n.r.*
11	Kaufmann	2006	Journal	number-size congruity task (Stroop-like)	Block design	17 (7)	English	9.6 (*n.r.*)	*n.r.*	right	I > N	n.r.	79
12	Kim-Spoon	2021	Journal	multi-source interference task	Block design	151 (n.r.)	English	16 (0.54)	13−17	*n.r.*	I > N	n.r.	398.4
13	Konrad	2005	Journal	Flanker task	Event-related design	16 (0)	English	10.1 (*n.r.*)	8−12	right	I > C	Yes	80
14	Liu	2016	Journal	multi-source interference task	Event-related design	72 (32)	English	13.9 (3.3)	8−19	*n.r.*	I > C	Yes	314
15	Margolis	2017	Journal	Simon task	Event-related design	55 (43)	English	16.1 (3.8)	7−22	*n.r.*	I > C	Yes	40
16	Mincic	2010	Journal	Stroop task	Event-related design	35 (17)	English	*n.r.*	16−17	right	I > N	*n.r.*	57.5
17	Posner	2011	Journal	Stroop task	Block design	15 (2)	English	13.4 (1.2)	11−16	right	I > N	*n.r.*	70.2
18	Puetz	2016	Journal	Stroop task	Block design	19 (n.r.)	English	12.9 (1.32)	10−14	*n.r.*	I > N	*n.r.*	100
19	Rubia	2006	Journal	Simon task	Event-related design	28 (0)	English	15 (2)	10−17	right	I > C	Yes	102
20	Schulte	2020	Journal	Stroop task	Block design	178 (91)	English	16 (2.3)	12−21	*n.r.*	I > C	*n.r.*	10.35
21	Sebastian	2021	Journal	Simon task	Block design	52 (0)	English	14 (1.68)	10−16	*n.r.*	I > C	n.r.	59
22	Sheridan	2014	Journal	Simon task	Block design	33 (14)	English	8.1 (1.66)	5.7−10.7	*n.r.*	I > C	*n.r.*	44
23	Tamm	2002	Journal	Stroop task	Event-related design	14 (14)	English	15.43 (3.79)	10−22	*n.r.*	I > N	n.r.	76.16
24	Vaidya	2005	Journal	Flanker task	Event-related design	10 (3)	English	9.2 (1.3)	7−11	*n.r.*	I > N	Yes	43.3
25	vantEnt	2009	Journal	Stroop & Flanker task	Event-related design	18 (10)	English	12 (*n.r.*)	7−12	*n.r.*	I > C	Yes	64.7
26	Wang	2009	Journal	Stroop task	Event-related design	group1: 22 (7)	English	15 (1.1)	13−17	*n.r.*	I > C	*n.r.*	29.7
27	Wang	2009	Journal	Stroop task	Event-related design	group2: 22 (4)	English	14.8 (1.2)	13−17	*n.r.*	I > C	*n.r.*	31.4
Young to middle-aged adults													
1	Aarts	2008	Journal	Stroop task	Event-related design	12 (10)	English	21.2 (*n.r.*)	18−24	right	I > C	Yes	94.85
2	Adleman	2002	Journal	Stroop task	Event-related design	11 (8)	English	19.98 (1.72)	17.39−22.68	right	I > C	*n.r.*	*n.r.*
3	Ansari	2006	Journal	number-size congruity task (Stroop-like)	Event-related design	14 (8)	English	21 (*n.r.*)	18−24	right	I > C	*n.r.*	38.4
4	Balodis	2013	Journal	Stroop task	Event-related design	21 (n.r.)	English	34.2(10.2)	19−64	*n.r.*	I > C	*n.r.*	218.46
5	Barros-Loscertales	2011	Journal	Stroop task	Block design	16 (n.r.)	English	34.2 (8.86)	*n.r.*	right	I > N	n.r.	55.12
6	Basten	2011	Journal	Stroop task	Event-related design	46 (22)	English	22.3 (2)	19−27	right	I > C	*Yes*	48.67
7	Brass	2005	Journal	Stroop task	Event-related design	20 (12)	English	26 (*n.r.*)	21−37	right	I > C	*n.r.*	163.1
8	Bunge	2002	Journal	Flanker task	Event-related design	16 (7)	English	27 (*n.r.*)	18−44	right	I > N	Yes	23
9	Bush	2003	Journal	multi-source interference task	Block design	8 (4)	English	30.4 (5.6)	*n.r.*	right	I > C	*n.r.*	308
10	Bush	1998	Journal	Stroop task	Block design	9 (4)	English	24.2 (2.3)	*n.r.*	right	I > N	*n.r.*	46

11	Carp	2012	Journal	multi-source interference task	Event-related design	21 (6)	English	39.8 (*n.r.*)	23−51	n.r.	I > C	Yes	237.3
12	Carter	1995	Journal	Stroop task	Event-related design	15 (8)	English	34.3 (*n.r.*)	22−49	right	I>C	No	236.6
13	Chen	2023	Journal	Stroop task	Event-related design	41 (22)	English	21.3 (2.8)	*n.r.*	right	I > C	yes	104
15	Christensen	2011	Journal	Stroop task	Event-related design	26 (16)	English	25.9 (*n.r.*)	19−53	right	I > N	Yes	38.5
16	Cieslik	2010	Journal	Stimulus–response compatibility task	Event-related design	24 (11)	English	29 (*n.r.*)	20−59	right	I > C	Yes	62.75
17	Coderre	2008	Journal	Stroop task	Block design	9 (7)	English	36 (9.4)	> = 18	right	I > C	*n.r.*	95.8
18	Cui	2011	Thesis	Stroop task	Event-related design	group1: 10 (9)	Chinese	21 (1.9)	18−28	right	I > C	*n.r.*	136
19	Cui	2011	Thesis	Stroop task	Event-related design	group2: 10 (0)	Chinese	22.4 (3.0)	18−28	right	I > C	*n.r.*	143
20	Dash	2019	Journal	Flanker task	Event-related design	20 (9)	English	32.6 (3.1)	*n.r.*	*n.r.*	I > C	Yes	67.27
21	DeVito	2012	Journal	Stroop task	Event-related design	12 (7)	English	31.0 (8.6)	18−50	right	I > C	No	1323
22	Durston	2003	Journal	Flanker task	Event-related design	9 (4)	English	25.7 (*n.r.*)	*n.r.*	right	I > C	Yes	64
23	Fan	2003	Journal	Flanker & Stroop & Spatial conflict task	Event-related design	12 (6)	English	24.7 (4.6)	18−34	right	I > C	n.r.	63
24	Fan	2008	Journal	Flanker task	Event-related design	16 (8)	English	27.2 (5.7)	18−36	right	I > C	Yes	101
25	Fan	2007	Journal	Flanker task	Event-related design	19 (9)	English	26 (*n.r.*)	18−59	*n.r.*	I > C	n.r.	61
26	Fechir	2010	Journal	Stroop task	Block design	16 (n.r.)	English	23.8 (1.4)	21−26	right	I > C	n.r.	70.1
27	Feola	2023	Journal	Simon task	Event-related design	77 (43)	English	31.75 (8.58)	22−50	n.r.	I > C	*n.r.*	63
28	Forstmann	2008	Journal	Simon task	Block design	24 (15)	English	24.2 (2.76)	*n.r.*	right	I > N	*n.r.*	21
29	Fruhholz	2011	Journal	Simon & Flanker task	Event-ralated design	24 (21)	English	23.91 (5.31)	18−43	right	I > C	Yes	45.7
30	George	1994	Journal	Stroop task	Event-related design	21 (10)	English	38.4 (13.2)	*n.r.*	right	I > N	*n.r.*	192
31	Georgiou-Karistianis	2012	Journal	Simon task	Event-related design	14 (5)	English	33.7 (7.9)	*n.r.*	right	I > C	*n.r.*	58
32	Grandjean	2013	Journal	Stroop task	Event-related design	25 (13)	English	21.8 (2.68)	18−29	right	I > C	Yes	182.05
33	Guo	2024	Journal	Flanker task	Event-related design	27 (14)	English	21.93 (2.35)	*n.r.*	right	I > C	yes	181
34	Harrison	2005	Journal	Stroop task	Hybrid block/Event-related design	9 (2)	English	27.4 (9.1)	*n.r.*	right	I > C	n.r.	181.1
35	Hazeltine	2003	Journal	Flanker task	Event-related design	10 (5)	English	27 (*n.r.*)	18−44	right	I > N	n.r.	46
36	Hazeltine	2000	Journal	Flanker task	Hybrid block/Event-related design	8 (5)	English	21 (*n.r.*)	18−24	right	I > C	*n.r.*	39
37	Ivanov	2012	Journal	Flanker task	Event-related design	16 (6)	English	30.63 (7.44)	21−45	right	I > C	Yes	55.05
38	Jiang	2014	Journal	Stroop & Simon task	Event-related design	21 (11)	English	21.3 (*n.r.*)	*n.r.*	*n.r.*	I > C	Yes	28.5
39	Kerns	2006	Journal	Simon task	Event-related design	26 (14)	English	24.2 (4.5)	18−36	right	I > C	Yes	16.8
40	Kerns	2005	Journal	Stroop task	Event-related design	13 (4)	English	36 (4.6)	*n.r.*	right	I > C	Yes	90.4
41	Kim	2012	Journal	Stroop task	Event-related design	16 (9)	English	23.6 (2.9)	18−35	right	I > C	Yes	84
42	Kim	2014	Journal	Stroop task	Event-related design	18 (8)	English	25.3 (3.6)	19−34	right	I > C	Yes	205.8
43	King	2012	Journal	Flanker task	Event-related design	25 (14)	English	23.8 (*n.r.*)	18−33	right	I > C	Yes	109
44	Korsch	2014	Journal	Simon & Flanker task	Event-related design	20 (10)	English	22.95 (2.72)	*n.r.*	right	I > C	Yes	35
45	Kozasa	2012	Journal	Stroop task	Block design	19 (10)	English	43.8 (9.35)	*n.r.*	right	I > C	n.r.	87.8
46	Krebs	2015	Journal	Stroop task	Event-related design	20 (12)	English	22.5 (*n.r.*)	18−35	both	I > (C+N)/2	n.r.	20.8
47	Laeng	2011	Journal	Stroop task	Hybrid block/Event-related design	10 (10)	English	53.8 (14)	*n.r.*	*n.r.*	I > C	*n.r.*	61.8
48	Li	2015	Journal	Simon task	Hybrid block/Event-related design	24 (11)	English	23 (3.26)	*n.r.*	right	I > C	Yes	116.25
49	Lutcke	2009	Journal	Flanker task	Event-related design	12 (9)	English	28 (6)	*n.r.*	right	I > C	Yes	66
50	Mathis	2009	Journal	Stroop task	Block design	12 (5)	English	26.8 (3.4)	22−30	*n.r.*	I > N & I > C	n.r.	60
51	Mathis	2009	Journal	Stroop task	Block design	12 (8)	English	51.7 (3.1)	46–55	*n.r.*	I > N & I > C	n.r.	63.5
52	Matthews	2004	Journal	Stroop task	Block design	18 (7)	English	39 (*n.r.*)	27−56	*n.r.*	I > C	*n.r.*	112
53	McNab	2008	Journal	Flanker task	Event-related design	11 (7)	English	24 (*n.r.*)	22−34	right	I > C	*n.r.*	30

54	Mead	2002	Journal	Stroop task	Block design	18 (10)	English	26.7 (*n.r.*)	18−46	right	I > C & I > N	*n.r.*	108
55	Milham	2002	Journal	Stroop task	Block design	12 (5)	English	23 (*n.r.*)	21−27	right	I > C & I > N	*n.r.*	147
56	Mitchell	2005	Journal	Stroop task	Block design	15 (11)	English	23.3 (6.31)	*n.r.*	right	I > N	*n.r.*	68
57	Mitchell	2010	Journal	Stroop task	Block design	28 (23)	English	20.2 (2.9)	*n.r.*	right	I > C	*n.r.*	82.5
58	moubochuan	2018	Thesis	Stroop task	Event-related design	37 (21)	Chinese	21.4 (1.4)	*n.r.*	right	I > C	Yes	32.5
59	Nakao	2005	Journal	Stroop task	Event-related design	14 (9)	English	30.2 (5.13)	24−43	both	I > C	*n.r.*	116
60	Ochsner	2009	Journal	Flanker task	Event-related design	16 (9)	English	21.22 (*n.r.*)	*n.r.*	right	I > C	Yes	33.9
61	Onur	2011	Journal	visual-spatial Stroop & Simon-like task	Event-related design	15 (6)	English	24.23 (3.09)	*n.r.*	right	I > C	*n.r.*	22
62	Page	2009	Journal	Stroop task	Event-related design	11 (0)	English	34.1 (10.1)	*n.r.*	right	I > C	Yes	120.1
63	Piai	2013	Journal	Stroop task	Event-related design	23 (12)	English	21.2 (*n.r.*)	18−29	right	I > C & I > N	Yes	75.5
64	Polosan	2011	Journal	Stroop task	Block design	14 (10)	English	35.9 (7.2)	*n.r.*	right	I > C	n.r.	113.23
65	Pompei	2011	Journal	Stroop task	Block design	45 (n.r.)	English	36.33 (12.8)	*n.r.*	*n.r.*	I > N	Yes	250
66	Prakash	2009	Journal	Stroop task	Event-related design	25 (n.r.)	English	23.6 (n.r.)	18−35	right	I > N	Yes	40.51
67	qianqiaoyun	2020	Journal	Stroop task	Block design	17 (9)	Chinese	25 (2)	22−28	right	I > C	*n.r.*	95.785
68	Rahm	2014	Journal	Stroop task	Block design	11 (3)	English	34.9 (7.8)	*n.r.*	right	I > N	*n.r.*	*n.r.*
69	Ravnkilde	2002	Journal	Stroop task	Event-related design	46 (30)	English	41 (11.6)	21−65	both	I > C	*n.r.*	292.3
70	Riva	2023	Journal	The finger-lifting task	Block design	29 (29)	English	24.52 (2.35)	21−31	right	I > C	*n.r.*	109
71	Rizio	2017	Journal	Stroop task	Event-related design	20 (n.r.)	English	23.7	18−31	right	I > N	Yes	106.5
72	Roberts	2008	Journal	Stroop task	Block design	16 (7)	English	24.3 (*n.r.*)	16−42	right	I > N	*n.r.*	60.5
73	Robertson	2015	Journal	number-size congruity task (Stroop-like)	Event-related design	16 (8)	English	23 (*n.r.*)	19−27	right	I > C	*n.r.*	56.01
74	Roelofs	2006	Journal	arrow word Stroop task	Event-related design	12 (8)	English	23 (*n.r.*)	21−28	right	I > C	No	44.05
75	Rubia	2006	Journal	Simon task	Event-related design	21 (0)	English	28 (6)	20−43	right	I > C	Yes	127
76	Schmidt	2012	Journal	Stroop task	Event-related design	31 (17)	English	24.125 (*n.r.*)	22−32	both	I > C	Yes	148.25
77	Schulze	2013	Journal	auditory Stroop task	Block design	8 (5)	English	24.8 (2)	22−27	right	I > C	n.r.	*n.r.*
78	Sebastian	2013	Journal	Simon task	Event-related design	48 (n.r.)	English	39.96 (17.14)	20−77	right	I > C	Yes	55.62
79	Sebastian	2012	Journal	Simon task	Event-related design	24 (13)	English	30.3 (8.1)	*n.r.*	right	I > C	Yes	60.18
80	Sebastian	2013	Journal	Simon task	Event-related design	24 (15)	English	27.42(5.6)	*n.r.*	right	I > C	Yes	58.19
81	Sheu	2012	Journal	Stroop & MSIT task	Block design	26 (12)	English	40 (6)	*n.r.*	*n.r.*	I > N	*n.r.*	*n.r.*
82	Soeda	2005	Journal	Stroop task	Block design	11 (4)	English	28.1 (4.7)	23−35	right	I > C	*n.r.*	*n.r.*
83	Sommer	2008	Journal	Simon task	Block design	12 (0)	English	29.1 (*n.r.*)	22−37	right	I > C	n.r.	86.5
84	Terry	2012	Journal	Stroop task	Event-related design	20 (0)	English	20.4 (1.6)	18−25	right	I > C	*n.r.*	76.81
85	Ullsperger	2001	Journal	Flanker task	Event-related design	9 (n.r.)	English	24.9 (*n.r.*)	21−29	right	I > C	Yes	61
86	Verdolini	2023	Journal	Stroop task	Block design	48 (28)	English	43.10 (8.61)	18−65	right	I > C	*n.r.*	65
87	Verstynen	2014	Journal	Stroop task	Event-related design	28 (n.r.)	English	31 (*n.r.*)	21−45	both	I > N	Yes	61.4
88	Wang	2023	Journal	Stroop task	Event-related design	50 (50)	English	22.78 (2.35)	*n.r.*	right	I > C	*n.r.*	38.5
89	Wittfoth	2006	Journal	Simon task	Event-related design	20 (17)	English	25.5 (*n.r.*)	21−31	*n.r.*	I > C	Yes	62
90	Wittfoth	2008	Journal	Simon task	Event-related design	15 (n.r.)	English	25.5 (*n.r.*)	21−31	right	I > C	Yes	56
91	Yang	2024	Journal	spatial Stroop-Simon task	Event-related design	33 (14)	English	21.5 (2.3)	19−28	right	I > C	*n.r.*	39.04
92	Ye	2009	Journal	Stroop & Flanker task	Event-related design	19 (12)	English	21 (*n.r.*)	19−23	right	I > C	Yes	77.5
93	Zhu	2010	Journal	Flanker task	Event-related design	22 (11)	English	20 (3)	*n.r.*	*n.r.*	I > C	Yes	130
94	Zoccatelli	2010	Journal	Stroop task	Block design	10 (2)	English	28 (*n.r.*)	22−40	right	I > C	n.r.	98.7

95	Zurawska	2011	Journal	Flanker task	Event-related design	18 (10)	English	25.3 (*n.r.*)	20−34	right	I > C	Yes	45
96	Zysset	2007	Journal	Stroop task	Event-related design	47 (24)	English	42 (*n.r.*)	22−75	*n.r.*	I > N	n.r.	90.3
The elderly													
1	Chuang	2014	Journal	Flanker task	Event-related design	60 (45)	English	64.6 (3.7)	60−74	right	I > C	Yes	60.75
2	Dash	2019	Journal	Flanker task	Event-related design	18 (n.r.)	English	73.94 (2.8)	*n.r.*	*n.r.*	I > C	Yes	49.44
3	Fernandez	2019	Journal	Flanker task	Event-related design	34 (n.r.)	English	72.7 (5.3)	*n.r.*	right	I > C	Yes	148.6
4	Gianaros	2007	Journal	Stroop task	Block design	46 (46)	English	68.04 (1.35)	*n.r.*	*n.r.*	I > C	*n.r.*	18.07
5	Gordon	2015	Journal	Stroop task	Event-related design	71 (44)	English	63.5 (*n.r.*)	49−78	right	I > C	*n.r.*	102
6	Huang	2012	Journal	physical Stroop task	Event-related design	18 (9)	English	66.07 (4.15)	61−73	right	I > C	Yes	107.5
7	Korsch	2014	Journal	Flanker & Simon task	Event-related design	19 (9)	English	70.26 (3.49)	*n.r.*	right	I > C	Yes	35
8	Mathis	2009	Journal	Stroop task	Block design	12 (3)	English	62.8 (3)	60−68	*n.r.*	I > N & I > C	n.r.	81
9	Milham	2002	Journal	Stroop task	Block design	10 (3)	English	68 (*n.r.*)	60−75	right	I > N & I > C	*n.r.*	220
10	Nagamatsu	2011	Journal	Flanker task	Event-related design	73 (73)	English	69.6 (3.1)	65−75	*n.r.*	I > C	n.r.	*n.r.*
11	Onur	2011	Journal	visual-spatial Stroop & Simon-like task	Event-related design	13 (5)	English	63.81 (6)	*n.r.*	right	I > C	*n.r.*	48.2
12	Prakash	2009	Journal	Stroop task	Event-related design	25 (n.r.)	English	65.5 (*n.r.*)	58−75	right	I > N	Yes	72.66
13	Puente	2014	Journal	Stroop task	Event-related design	26 (16)	English	74 (5.5)	65−85	both	I > C	Yes	247.1
14	Rizio	2017	Journal	Stroop task	Event-related design	20 (n.r.)	English	67 (*n.r.*)	60−79	right	I > N	Yes	80.77
15	Schultz	2024	Journal	color-word Stroop task	Event-related design	41 (n.r.)	English	66.63 (4.7)	60−77	right	I > C	yes	223.2
16	Won	2019	Journal	Flanker task	Event-related design	32 (24)	English	66.2 (7.3)	55−80	right	I > C	Yes	85.2
17	Zhu	2010	Journal	Flanker task	Event-related design	22 (13)	English	74 (6)	*n.r.*	*n.r.*	I > C	Yes	206

Note. *n.r.* = not reported; I = incongruent condition; C = congruent condition; N = neutral condition; RT = reaction time.